

# Ph<sub>2</sub>PCH<sub>2</sub>CH<sub>2</sub>B(C<sub>8</sub>H<sub>14</sub>) and Its Formaldehyde Adduct as Catalysts for the Reduction of CO<sub>2</sub> with Hydroboranes

Alberto Ramos,\* Antonio Antiñolo, Fernando Carrillo-Hermosilla, and Rafael Fernández-Galán

Cite This: <https://dx.doi.org/10.1021/acs.inorgchem.0c01152>

Read Online

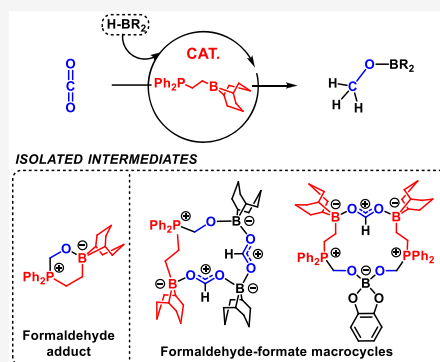
ACCESS |

Metrics & More

Article Recommendations

Supporting Information

**ABSTRACT:** We study two metal-free catalysts for the reduction of CO<sub>2</sub> with four different hydroboranes and try to identify mechanistically relevant intermediate species. The catalysts are the phosphinoborane Ph<sub>2</sub>P(CH<sub>2</sub>)<sub>2</sub>BBN (1), easily accessible in a one-step synthesis from diphenyl(vinyl)phosphine and 9-borabicyclo[3.3.1]nonane (H-BBN), and its formaldehyde adduct Ph<sub>2</sub>P(CH<sub>2</sub>)<sub>2</sub>BBN(CH<sub>2</sub>O) (2), detected in the catalytic reduction of CO<sub>2</sub> with 1 as the catalyst but properly prepared from compound 1 and *p*-formaldehyde. Reduction of CO<sub>2</sub> with H-BBN gave mixtures of CH<sub>2</sub>(OBBN)<sub>2</sub> (A) and CH<sub>3</sub>OBBN (B) using both catalysts. Stoichiometric and kinetic studies allowed us to unveil the key role played in this reaction by the formaldehyde adduct 2 and other formaldehyde–formate species, such as the polymeric BBN(CH<sub>2</sub>)<sub>2</sub>(Ph<sub>2</sub>P)(CH<sub>2</sub>O)BBN(HCO<sub>2</sub>) (3) and the bisformate macrocycle BBN(CH<sub>2</sub>)<sub>2</sub>(Ph<sub>2</sub>P)(CH<sub>2</sub>O)BBN(HCO<sub>2</sub>)BBN(HCO<sub>2</sub>) (4), whose structures were confirmed by diffractometric analysis. Reduction of CO<sub>2</sub> with catecholborane (HBcat) led to MeOBcat (C) exclusively. Another key intermediate was identified in the reaction of 2 with the borane and CO<sub>2</sub>, this being the bisformaldehyde–formate macrocycle (HCO<sub>2</sub>)<sub>2</sub>{BBN(CH<sub>2</sub>)<sub>2</sub>(Ph<sub>2</sub>P)(CH<sub>2</sub>O)}<sub>2</sub>Bcat (5), which was also structurally characterized by X-ray analysis. In contrast, using pinacolborane (HBpin) as the reductant with catalysts 1 and 2 usually led to mixtures of mono-, di-, and trihydroboration products HCO<sub>2</sub>Bpin (D), CH<sub>2</sub>(OBpin)<sub>2</sub> (E), and CH<sub>3</sub>OBpin (F). Stoichiometric studies allowed us to detect another formaldehyde–formate species, (HCO<sub>2</sub>)BBN(CH<sub>2</sub>)<sub>2</sub>(Ph<sub>2</sub>P)(CH<sub>2</sub>O)Bpin (6), which may play an important role in the catalytic reaction. Finally, only the formaldehyde adduct 2 turned out to be active in the catalytic hydroboration of CO<sub>2</sub> using BH<sub>3</sub>·SMe<sub>2</sub> as the reductant, yielding a mixture of two methanol-level products, [(OMe)BO]<sub>3</sub> (G, major product) and B(OMe)<sub>3</sub> (H, minor product). In this transformation, the Lewis adduct (BH<sub>3</sub>)Ph<sub>2</sub>P(CH<sub>2</sub>)<sub>2</sub>BBN was identified as the resting state of the catalyst, whereas an intermediate tentatively formulated as the Lewis adduct of compound 2 and BH<sub>3</sub> was detected in solution in a stoichiometric experiment and is likely to be mechanistically relevant for the catalytic reaction.



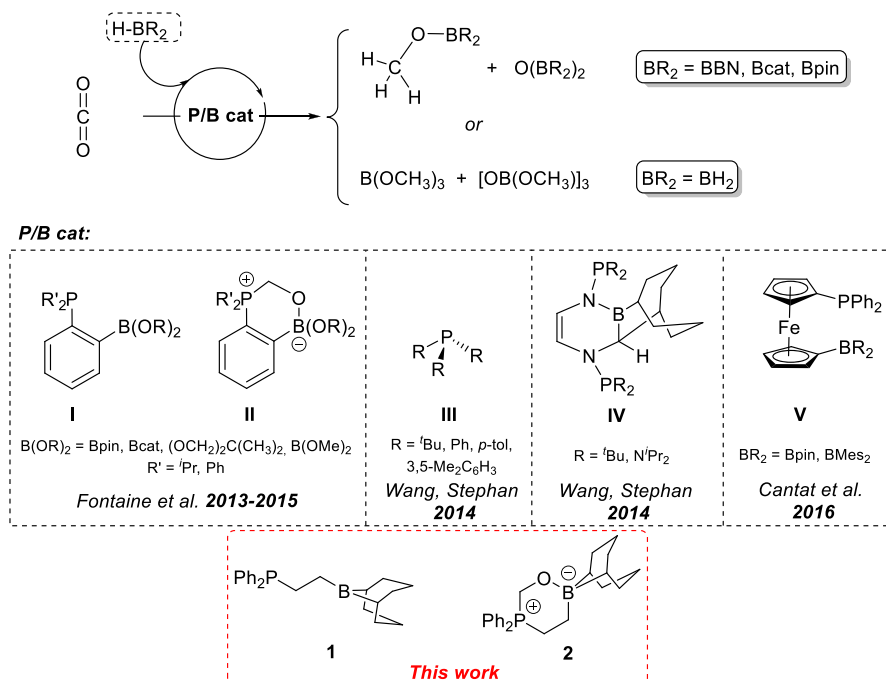
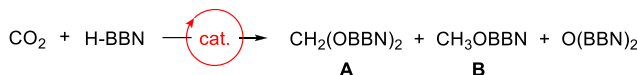
## INTRODUCTION

In the last decades, there has been increasing concern among the scientific community to develop more efficient CO<sub>2</sub> capture and conversion technologies in order to reduce the concentration of greenhouse gas in the atmosphere and, at the same time, use it as a C1 feedstock for value-added chemicals.<sup>1</sup> One of the most interesting and challenging transformations to achieve is an efficient six-electron reduction of captured CO<sub>2</sub> to produce methanol, which could then be used as a fuel. This is the paradigm of a circular economy coined as “Methanol Economy”, initially proposed by Olah and collaborators.<sup>2</sup> From an industrial point of view, hydrogen would be the ideal reductant, generating water as the only byproduct. However, only a few homogeneous catalysts based on transition metals have been reported to date for the aforementioned transformation, operating under harsh reaction conditions, with low efficiencies and usually requiring stoichiometric amounts of additives.<sup>3</sup> Alternatively, hydroboranes<sup>4</sup> and hydrosilanes<sup>4a,e,i,5</sup> can also be employed as reductants. Although less appealing from an industrial point of view because of the generation of undesired B- or Si-containing byproducts, their use allows, in

turn, milder reaction conditions (25–90 °C, 1–5 atm of CO<sub>2</sub>), which facilitate monitoring of the reactions to gain valuable mechanistic information and even enable the use of metal-free catalysts.<sup>4b,d,f,i</sup>

Turning our attention to the catalytic hydroboration of CO<sub>2</sub> to the methanol level, Guan and co-workers reported the first example back in 2010, using a Ni complex with a pincer ligand and catecholborane (HBcat) as the reductant.<sup>6</sup> In 2013, Fontaine and co-workers reported the first example of a metal-free catalyst for the reduction of CO<sub>2</sub> to the methanol level using an ambiphilic phosphinoboronate catalyst (I in Scheme 1) and up to four different commercial hydroboranes: HBcat, pinacolborane (HBpin), 9-borabicyclo[3.3.1]nonane (H-

Received: April 21, 2020

Scheme 1. P/B-Containing Catalysts for the Reduction of CO<sub>2</sub> to the Methanol Level with HydroboranesTable 1. Catalytic Hydroboration of CO<sub>2</sub> with HBBN<sup>a</sup>

entry	catalyst	cat. load (mol %)	T (°C)	t (h)	conv (%) <sup>b</sup>	TON <sup>c</sup> A	TON <sup>c</sup> B
1	Ph <sub>2</sub> PCHCH <sub>2</sub>	1	25	22	>99	5.0	92.0
2	Ph <sub>2</sub> PCHCH <sub>2</sub>	2.5	60	0.5	47	9.6	6.6
3	Ph <sub>2</sub> PCHCH <sub>2</sub>	2.5	60	1	80	14.6	14.3
4	Ph <sub>2</sub> PCHCH <sub>2</sub>	1	60	3	100	14.8	64.6
5	Ph <sub>2</sub> PCHCH <sub>2</sub>	0.1	60	1	51	220.5	228.5
6	Ph <sub>2</sub> PCHCH <sub>2</sub>	0.1	60	12	83		663.0
7	Ph <sub>2</sub> PCHCH <sub>2</sub>	0.05	60	1	40	263.0	322.0
8	Ph <sub>2</sub> PCHCH <sub>2</sub>	0.05	60	16	63	15.0	764.0
9	<b>1</b>	1	25	20	100	9.5	91.4
10	<b>1</b>	2.5	60	0.5	50	8.9	9.2
11	<b>1</b>	2.5	60	1	82	9.6	19.0
12	<b>1</b>	1	60	3	>99	6.6	70.8
13	<b>1</b>	0.1	60	1	23	77.0	167.0
14	<b>1</b>	0.1	60	7	45	9.5	324.0
15	<b>2</b>	1	25	12	100	1.1	92.3
16	<b>2</b>	2.5	60	0.2	60	14.5	8.8
17	<b>2</b>	2.5	60	0.5	>99	16.1	17.1
18	<b>2</b>	1	60	3	98	18.0	71.0
19	<b>2</b>	0.1	60	1	37	97.5	177.0
20	<b>2</b>	0.1	60	7	63	17.5	341.0

<sup>a</sup>Reaction conditions: J. Young valve NMR tube containing ca. 0.6 mL C<sub>6</sub>D<sub>6</sub> solutions of H-BBN (0.2 mmol), catalyst and internal standard [Si(SiMe<sub>3</sub>)<sub>4</sub>, 0.01 mmol], and CO<sub>2</sub> (1 atm). <sup>b</sup>Based on the relative integrals of H-BBN and products in the <sup>11</sup>B NMR. <sup>c</sup>Calculated according to the number of C–H bonds formed in the reduction products by integration of the corresponding signals relative to the internal standard in the <sup>1</sup>H NMR spectra.

BBN), and BH<sub>3</sub>·SMe<sub>2</sub>.<sup>7</sup> Since then, a limited number of metal-free catalysts have been reported, mostly involving strong bases or ambiphilic species.<sup>7,8</sup> Among them, a few phosphinoborane systems turned out to be efficient, easily accessible catalysts for this reaction. As mentioned above, Fontaine and co-workers developed a series of phosphinoborane catalysts, which

turned out to be very active,<sup>7,8g,i</sup> especially when using BH<sub>3</sub> as the reductant. Mechanistic studies revealed the crucial role of the formaldehyde adducts of phosphineboronate species (**II** in Scheme 1)<sup>8g</sup> detected during the catalysis that, when used as catalysts themselves, eliminated the induction period previously observed for the reactions catalyzed by the parent

phosphinoboranes. Wang and Stephan reported that simple phosphines (**III** in Scheme 1) were capable of reducing CO<sub>2</sub> to a mixture of boron formate, acetal, and boron methoxide using H-BBN as both the reductant and Lewis acid counterpart for the phosphine to form an intermolecular frustrated Lewis pair (FLP).<sup>8i</sup> The same authors also reported intramolecular P/B FLPs, generated by ring expansion in the reactions of phosphine-derived carbenes and H-BBN (**IV** in Scheme 1) as active catalysts on the reduction of CO<sub>2</sub> with HBpin, HBCat, and BH<sub>3</sub>·SMe<sub>2</sub>.<sup>8h</sup> Finally, Cantat and co-workers reported the synergistic effects of ferrocene-based phosphinoboranes (**V** in Scheme 1) in the catalytic reduction of CO<sub>2</sub> to the methoxide level with H-BBN.<sup>9</sup>

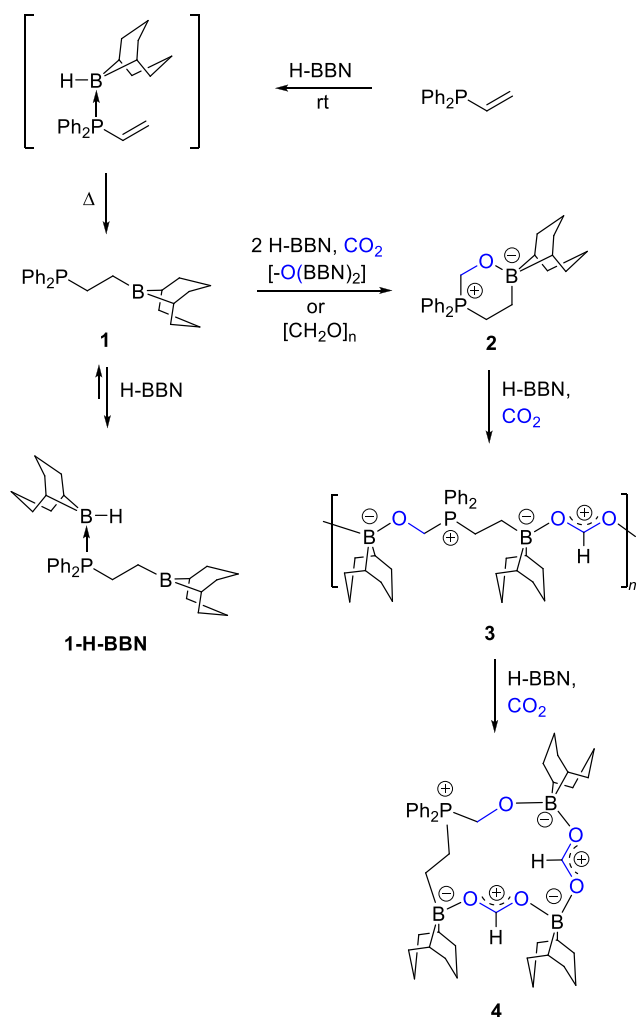
In order to fill the gap left by the phenylene and ferrocenylene phosphinoboranes, we decided to focus on a simpler ethylene-linked phosphinoborane, Ph<sub>2</sub>P(CH<sub>2</sub>)<sub>2</sub>BBN (**1**),<sup>10</sup> easily accessible in an atom-economical uncatalyzed process from commercial reagents (Ph<sub>2</sub>PCHCH<sub>2</sub> and H-BBN), which, to our knowledge, had not been tested as a catalyst for hydroboration of CO<sub>2</sub>. We also used the four most common commercial hydroboranes as reductants—H-BBN, HBCat, HBpin, and BH<sub>3</sub>·SMe<sub>2</sub>—obtaining in most cases methoxide derivatives as the major (or only) reduction products. Additionally, the formaldehyde adduct Ph<sub>2</sub>P-(CH<sub>2</sub>)<sub>2</sub>BBN(CH<sub>2</sub>O) (**2**), detected as an intermediate in the catalytic reduction with H-BBN, was tested as a catalyst as well with all of the different boranes. Stoichiometric and kinetic experiments helped us to identify other important intermediates and gain some mechanistic insights for these transformations. These studies not only confirmed the crucial role played by the formaldehyde adduct **2** but also that of other formaldehyde–formate derivatives detected during the catalysis, some of them structurally characterized for the first time.

## ■ RESULTS AND DISCUSSION

**Catalytic Reduction of CO<sub>2</sub> with HBBN.** As stated above, we synthesized the phosphinoborane **1** according to a slightly modified literature procedure,<sup>10</sup> by the direct reaction of equimolar amounts of Ph<sub>2</sub>PCHCH<sub>2</sub> and H-BBN in toluene at 100 °C for 3 h. Compound **1** was isolated in very good yields (up to 76%, ca. 0.5 g), and its NMR characterization matched well with the reported data in the literature, so no further comments in this respect will be made (see the Supporting Information). Because H-BBN reacts directly with Ph<sub>2</sub>PCHCH<sub>2</sub>, even at room temperature (slowly), we decided to test initially both diphenyl(vinyl)phosphine (entries 1–8, Table 1) and compound **1** (entries 9–14, Table 1) for the reduction of CO<sub>2</sub> with H-BBN. As can be seen in Table 1, the results and trends found after modification of the time, temperature, and catalyst loads for both catalysts were rather similar. Thus, in all instances, mixtures of the double and triple hydroboration products, the acetal CH<sub>2</sub>(OBBN)<sub>2</sub> (**A**) and the methoxide CH<sub>3</sub>OBBN (**B**), were obtained in different proportions, with **B** being favored at long reaction times and lower catalyst loadings, in good agreement with the results reported with phosphines as catalysts.<sup>8i</sup> In contrast, the formate derivative, HCO<sub>2</sub>BBN, was never detected. As expected, for the same catalyst load, increasing temperature also decreased the reaction time (i.e., total consumption of borane took roughly 1 day at 25 °C but only 3 h at 60 °C at 1 mol % catalyst load). In terms of activity, we noticed slightly better results with diphenyl(vinyl)phosphine because catalysts loads down to 0.05 mol % were tolerated and a total turnover

number (TON) of 779 was measured after 12 h at 60 °C (63% of the borane consumed, entry 8), whereas a more pronounced activity decay was observed for compound **1** at 0.1 mol % load (entry 14). Another interesting trend observed in the reactions conducted at 60 °C, especially at lower catalyst loads, was the dramatic activity decay after 1 h (i.e., the total TON is already 585 at a catalyst load of 0.05 mol % after 1 h in entry 7), suggesting catalyst deactivation, which will be commented on in more detail in the kinetic studies section.

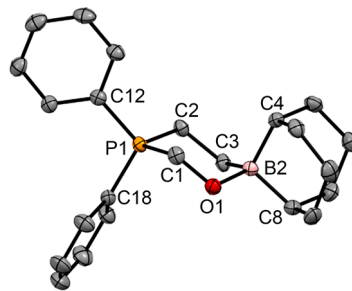
**Stoichiometric Reactions with H-BBN and CO<sub>2</sub>.** In order to ascertain the transformations undergone by the catalyst during the hydroboration reaction and identify possible intermediates or active species involved during the catalysis, we monitored the reaction using 5 mol % Ph<sub>2</sub>PCHCH<sub>2</sub> as the catalyst by multinuclear NMR and were able to detect several species. Initially, after 20 min under a CO<sub>2</sub> atmosphere (1 atm) at 25 °C, we detected what we propose to be the diphenyl(vinyl)phosphine–H-BBN adduct, with signature signals in the <sup>31</sup>P and <sup>11</sup>B NMR at δ<sub>p</sub> 5.3 ppm and δ<sub>B</sub> –13.7 ppm, respectively, which was also observed as an intermediate in the preparation of the phosphinoborane **1** reported by Tilley and collaborators.<sup>10c</sup> Further confirmation of this hypothesis came from the presence of three multiplets in the <sup>1</sup>H NMR spectrum between δ<sub>H</sub> 5.1 and 6.5 ppm attributed to the three vinylic protons. Interestingly, no traces of the reduction products, the acetal **A** or the methoxide **B**, were detected in the latter spectrum. The sample was then heated at 60 °C for 1.5 h, depleting most of the borane (89% consumption by <sup>11</sup>B NMR) and forming substantial amounts of **A** and **B**. The initial diphenyl(vinyl)phosphine–H-BBN adduct had completely disappeared, and the main active species was the new adduct (H-BBN)Ph<sub>2</sub>P(CH<sub>2</sub>)<sub>2</sub>BBN (**1-H-BBN**). The nature of **1-H-BBN** was fully confirmed by the stoichiometric reaction between compound **1** and H-BBN at room temperature (Scheme 2), slowly reaching an equilibrium after 24 h, which is clearly shifted toward the adduct (ratio of ca. 9:1 **1-H-BBN**/**1**). The NMR characterization of this independently prepared solution of **1-H-BBN** matched nicely with the signals observed in the previous spectra during the catalytic reaction, with those of the <sup>31</sup>P and <sup>11</sup>B NMR spectra, at δ<sub>p</sub> 8.4 ppm and δ<sub>B</sub> 86.1 and –15.1 ppm, the latter two ascribed to tri- and tetracoordinated boron, respectively, being the most revealing. The initial sample was further heated at 60 °C for a total time of 2.3 h until full consumption of H-BBN. At this point, a new intermediate was detected and postulated as the formaldehyde adduct Ph<sub>2</sub>P(CH<sub>2</sub>)<sub>2</sub>BBN(CH<sub>2</sub>O) (**2**; Scheme 2), with signals at δ<sub>p</sub> –0.4 ppm and δ<sub>B</sub> –1.2 ppm, respectively, and a diagnostic doublet at ca. δ<sub>H</sub> 4.8 ppm (<sup>2</sup>J<sub>PH</sub> ≈ 2 Hz) for methylene protons of the formaldehyde unit in the <sup>1</sup>H NMR spectrum. Compound **2** could be selectively prepared from **1** and *p*-formaldehyde, and its full characterization in both solution and solid state will be commented on later. Finally, right after the addition of more H-BBN and repressurization with CO<sub>2</sub>, we detected a new species with signature signals at δ<sub>p</sub> 26.0 ppm and δ<sub>H</sub> 8.74 and 4.63 ppm, respectively, assigned to the formate (HCO<sub>2</sub>) and formaldehyde (CH<sub>2</sub>O) units, which could be identified after independent stoichiometric reactions (vide infra) as the macrocyclic compound BBN(CH<sub>2</sub>)<sub>2</sub>(Ph<sub>2</sub>P)(CH<sub>2</sub>O)BBN-(HCO<sub>2</sub>)BBN(HCO<sub>2</sub>) (**4**; Scheme 2), with two formate moieties and one formaldehyde group. Further monitoring of this reaction for 24 h at room temperature led again to depletion of the borane and full transformation into the

**Scheme 2.** General Reactivity of  $\text{Ph}_2\text{PCHCH}_2$  toward H-BBN and  $\text{CO}_2$ 

hydroboration products **A** (minor) and **B** (major), whereas compound **4** remained as the only active species detected in solution. It should also be mentioned that, in a separate experiment, we tested the lack of reactivity of phosphineborane **1** toward  $\text{CO}_2$ , in agreement with the experimental and computational results reported by Fontaine and co-workers for related phosphineboronate derivatives.<sup>7,8g,l</sup>

Formation of the formaldehyde adduct **2** can be explained by the reaction of the phosphineborane **1** with the acetal **A** originating from double hydroboration of  $\text{CO}_2$  with H-BBN catalyzed by **1** itself. As previously computed by Fontaine, bisboryl acetal species may be in equilibrium with free formaldehyde and bisboryl ether.<sup>8l</sup> Thus, free formaldehyde would be immediately trapped by the ambiphilic P/B system (in our case, compound **1**) to give a formaldehyde adduct. Evidence, and subsequent trapping, of transient formaldehyde was also provided by Sabo-Etienne and co-workers using Ru catalysts and HBcat as the reductant.<sup>11</sup> However, a more convenient and efficient approach to prepare **2**, as stated above, involves the use of *p*-formaldehyde  $[\text{CH}_2\text{O}]_n$ , a synthetic route also employed by Fontaine and co-workers to prepare formaldehyde adducts of phosphineboronates of the formula  $o\text{-(C}_6\text{H}_4\text{)}(\text{PPh}_2)[\text{B}(\text{OR})_2]$ .<sup>8g,l</sup> Thus, mild heating (60 °C) of suspensions containing **1** and *p*-formaldehyde led to

compound **2** in very good yields (up to 89%, 0.33 g). The structure of compound **2** was unambiguously established after X-ray diffraction analysis of a single crystal (Figure 1).

**Figure 1.** Molecular structure of compound **2** with ellipsoids at 30% probability level and H atoms omitted for clarity. Only one of the two crystallographically independent molecules found in the asymmetric unit is shown. Selected bond lengths (Å) and angles (deg): C1–O1 1.387(3), O1–B2 1.550(3), B2–C3 1.624(3), C3–C2 1.522(3), C2–P1 1.793(2), P1–C1 1.829(2); C3–B2–O1 106.7(2), C1–P1–C2 104.9(1), C12–P1–C18 110.0(1), C4–B2–C8 104.8(2), C1–C2–C3–O1 2.13(8).

Compound **2** crystallized in the triclinic space group  $P\bar{1}$ , with two crystallographically independent molecules in the asymmetric unit, essentially with the same parameters, so only one of them will be discussed. As can be seen, compound **2** is a six-membered zwitterionic heterocycle with a chair conformation. The  $\text{PPh}_2$  and BBN groups are linked together by ethylene ( $\text{CH}_2\text{CH}_2$ ) and formaldehyde ( $\text{CH}_2\text{O}$ ) units, which display roughly a planar arrangement, as denoted by a C1–C2–C3–O1 torsion angle of only  $2.13(8)^\circ$ , with the P and B atoms folding out of this plane in an almost antiparallel disposition. These two atoms also display somewhat distorted tetrahedral coordination geometries, as expected for phosphonium/borate groups. Two new single P–C and O–B bonds have been formed, as denoted by the corresponding P1–C1 and O1–B2 distances, of 1.829(2) and 1.550(3) Å, respectively. The chair arrangement of the heterocycle differs from that of the formaldehyde adduct of  $o\text{-(C}_6\text{H}_4\text{)}(\text{PPh}_2)\text{-(Bcat)}$ ,<sup>8l</sup> which shows a half-chair conformation similar to that of cyclohexene.

The NMR spectra for compound **2** are consistent with the solid-state structure allowing the usual dynamic processes, fast in the NMR time scale, such as free rotation of Ph rings or chair flipping, which give rise to an apparent symmetry plane that accounts for the presence of five signals for the BBN group and four signals for the Ph groups in the  $^{13}\text{C}$  NMR spectrum. The formaldehyde moiety was evident in the  $^1\text{H}$  and  $^{13}\text{C}$  NMR spectra with the presence of two doublets, at 4.87 and 60.4 ppm ( $^1J_{\text{PC}} = 47.5$  Hz), respectively. The signals in the  $^{31}\text{P}$  and  $^{11}\text{B}$  NMR spectra match well with those found in the catalytic reaction commented on above and will not be further discussed. Because formaldehyde adducts of ambiphilic species have been proven to play a key role as catalysts for the hydroboration of  $\text{CO}_2$ , as shown by us (boron amidinate system)<sup>8a</sup> and Fontaine and co-workers (phosphineboronate compounds),<sup>8g,l</sup> we also decided to test compound **2** as the catalyst for hydroboration of  $\text{CO}_2$  with all of the boranes used in this study. In the first place, the results obtained were similar to those obtained for compound **1** when H-BBN was used as the reductant (entries 15–20, Table 1), but shorter reaction times were often required for reaction completion, especially at



25 °C (only 12 h, entry 15). A more detailed analysis accounting for these results will be given in the next section, discussing the kinetic studies.

The formation of compound **4** formally requires the capture of two boron formate units derived from the monohydroboration of CO<sub>2</sub> by H-BBN by the formaldehyde adduct **2** (Scheme 2). In order to prove this hypothesis, several stoichiometric experiments were carried out. In the first place, we mixed equimolar amounts of **2** and H-BBN in a C<sub>6</sub>D<sub>6</sub> solution and exposed the mixture to a CO<sub>2</sub> atmosphere (ca. 1 bar) at room temperature in an NMR tube. Monitoring the reaction, we noticed that new signals due to species still containing a formaldehyde group ( $\delta_{\text{H}}$  ca. 4.6 ppm) and a formate group ( $\delta_{\text{H}}$  ca. 8.7 ppm) appeared in the <sup>1</sup>H NMR spectra, which were also associated with two new broad signals in the <sup>31</sup>P NMR spectra at 25.8 and 24.2 ppm. Interestingly, the integral ratio of the formaldehyde/formate signals in the <sup>1</sup>H NMR spectra was neither 2:1, as would be expected for a species containing one unit of each group, nor 1:1, as would be expected for a species with two (equivalent) formate groups and one formaldehyde. Instead, the relative integral ratio takes an intermediate value that decreases as the reaction progresses: 2:1.4 after 20 min and 2:1.7 after 15 h. A parallel intensity increase of the signal at 25.8 ppm with respect to the one at 24.2 ppm was also noticed in the <sup>31</sup>P NMR spectra. This evidence led us to propose that up to two species, one bearing one formate group, BBN(CH<sub>2</sub>)<sub>2</sub>(Ph<sub>2</sub>P)(CH<sub>2</sub>O)BBN(HCO<sub>2</sub>) (**3**), and the other bearing two formate groups, **4**, were present in solution (Scheme 2). Compound **3** progressively crystallized from the latter mixture from the early stages of the reaction (vide infra), but its almost negligible solubility after crystallization precluded solution NMR characterization. After 15 h, apart from small amounts of **3** and **4**, only traces of compound **2** and the boron methoxide **B** are present in solution. The fact that only one set of signals was observed in the <sup>1</sup>H NMR spectra for the formaldehyde and formate groups of compounds **3** and **4**, together with the presence of two broad signals in the <sup>31</sup>P NMR spectra of these two compounds, might be due to rapid dissociation/coordination equilibria in solution of the boron formate units both within and between compounds **3** and **4**. Unfortunately, the extremely low solubility of both species in the usual organic solvents precluded a variable-temperature NMR study to support our hypothesis. In order to attest that the formate units came from CO<sub>2</sub>, the experiment was reproduced using <sup>13</sup>CO<sub>2</sub>, and a doublet in the <sup>1</sup>H NMR spectrum at 8.76 ppm (<sup>1</sup>J<sub>CH</sub> = 206.9 Hz), together with a broad signal in the <sup>13</sup>C NMR spectrum at 172.5 ppm, was easily attributed to the H<sup>13</sup>CO<sub>2</sub> groups of <sup>13</sup>C-**3** and <sup>13</sup>C-**4**. Small amounts of <sup>12</sup>CH<sub>3</sub>OBBN (**B**) were also detected in the <sup>1</sup>H and <sup>11</sup>B NMR spectra. The absence of an isotopically enriched product (<sup>13</sup>C-**B**) suggests that direct hydroboration of the formaldehyde unit in **2** also competes with the formation of **3** and **4**, but the reaction is much slower at room temperature, favoring the formation of **3** and **4**. In order to obtain compound **4** selectively, we decided to carry out a stoichiometric reaction involving 2 equiv of H-BBN, compound **2** and CO<sub>2</sub>. Again, monitoring the reaction by NMR spectroscopy revealed the progressive formation of compounds **3** and **4** in solution from the early stages of the reaction. Finally, after 3 days at room temperature, only compound **4** and the boron methoxide **B** remained in solution alongside a considerable amount of crystalline precipitate of **4**. As expected, the integral ratio between HCO<sub>2</sub> and H<sub>2</sub>CO

signals for compound **4** in the <sup>1</sup>H NMR spectrum was roughly 1:1, and a sharp signal in the <sup>31</sup>P NMR spectrum at 26.0 ppm was also attributed to **4**.

Definitive structural confirmation for compounds **3** and **4** came from diffractometric studies. Fortunately, single crystals of **3** for an X-ray diffraction analysis could be obtained from the first stoichiometric reaction. Compound **3** crystallized in the monoclinic *P*2<sub>1</sub>/*c* space group, displaying a polymeric structure with a helical arrangement and a pseudo-C<sub>2</sub> symmetry (Figures 2 and S32). As can be seen, the structure

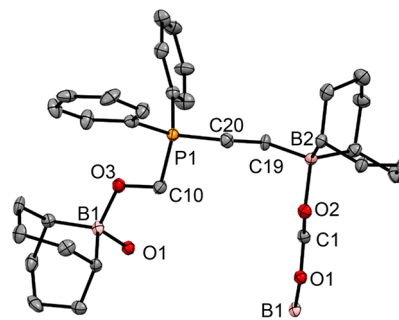


**Figure 2.** Molecular structure of compound **3** (polymeric structure), with ellipsoids at the 30% probability level and H atoms omitted for clarity. Selected bond lengths (Å) and angles (deg): B1–O1 1.621(6), B1–O3 1.495(7), O1–C1 1.264(5), C1–O2 1.256(6), O2–B2 1.630(5), B2–C19 1.608(6), C19–C20 1.518(7), C20–P1 1.801(5), P1–C10 1.812(5), C10–O3 1.401(6); O1–B1–O3 105.4(4), O1–C1–O2 120.8(4), O2–B2–C19 104.8(3), C10–P1–C20 106.2(2).

of **3** can be constructed from that of **2** after cleavage of the O → B dative bond, followed by the attachment of another BBN fragment to the O atom (O3 in Figure 2) and a formate group (HCO<sub>2</sub>) to the original BBN moiety present in **2**. This would leave a tricoordinate B atom (B1) with unquenched Lewis acidity, which accounts for the polymeric structure found in the solid state by donor–acceptor interactions with the O atom of a formate unit from a different monomer (O1). This type of polymeric structure in BBN derivatives is not unusual. In fact, the parent phosphinoborane **1** also forms a polymeric framework with P–B interactions in the solid state, accounting as well for its low solubility.<sup>10c</sup> As a consequence of this polymeric structure and the dative O → B bond formed, there is a symmetric charge delocalization in the formate unit, with almost identical C–O bond distances of ca. 1.26 Å, similar to the values measured for the macrocyclic tetramer [HCO<sub>2</sub>BBN]<sub>4</sub>.<sup>12</sup> Interestingly, the B–O distances between the formate unit and the BBN groups are slightly longer (ca. 1.63 Å) than those found in the mentioned formate tetramer,<sup>12</sup> the formaldehyde–formate zwitterions R<sub>3</sub>P(CH<sub>2</sub>O)BBN–(O<sub>2</sub>CH) (R = <sup>t</sup>Bu, *p*-C<sub>6</sub>H<sub>4</sub>Me)<sup>8i</sup> or related BBN carboxylate derivatives (1.53–1.59 Å).<sup>13</sup> This is indicative of weak O → B dative interactions<sup>13</sup> and may account for the proposed formate cleavage and rearrangement equilibria proposed in solution for **3** and **4**.

Crystals of compound **4** were grown from a reaction crude in toluene at –20 °C under a CO<sub>2</sub> atmosphere. It crystallized in the monoclinic *P*2<sub>1</sub>/*c* space group as a 14-membered zwitterionic macrocycle (Figure 3), as opposed to the open-chain polymeric structure displayed by compound **3**. The tendency of boron formate derivatives to form macrocycles in the solid state was already evident in HCO<sub>2</sub>BBN itself, which crystallized as a 16-membered macrocycle tetramer.<sup>12</sup> In fact,

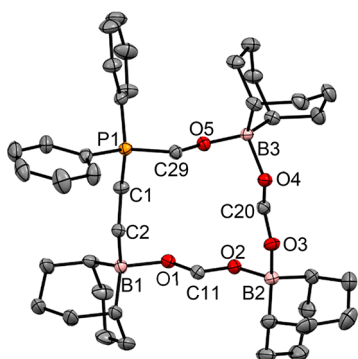


**Figure 3.** Molecular structure of compound **4**, with ellipsoids at the 30% probability level and H atoms and solvent molecules (toluene) omitted for clarity. Selected bond lengths (Å) and angles (deg): B1–O1 1.668(3), O1–C11 1.236(3), C11–O2 1.267(3), O2–B2 1.550(3), B2–O3 1.571(3), O3–C20 1.251(3), C20–O4 1.243(3), O4–B3 1.661(3), B3–O5 1.479(3), C29–O5 1.405(3); O5–B3–O4 102.6(2), O4–C20–O3 123.1(2), O3–B2–O2 103.9(2), O2–C11–O1 121.9(2), O1–B1–C2 102.2(2), C1–P1–C29 109.3(1).

the macrocycle of **4** is made up of two  $\text{HCO}_2\text{BBN}$  units linked together, trapped by the formaldehyde adduct **2** after cleavage of the  $\text{O} \rightarrow \text{B}$  dative bond. All three B atoms (borate groups), as well as the P atom (phosphonium group), display tetrahedral coordination environments. There is significant charge delocalization within the formate groups, more symmetrically in the O4–C20–O3 unit, with distances of 1.243(3) and 1.251(3) Å, whereas there is slightly more double-bond character for the C11–O1 couple [1.236(3) Å] than for the other pair, C11–O2 [1.267(3) Å], in the other formate group. Two of the B–O bonds between two of the BBN groups and the formate fragments are significantly elongated (B1–O1 and B3–O4 of ca. 1.66 Å), even more so than those of compound **3**, implying even weaker  $\text{O} \rightarrow \text{B}$  dative interactions. However, the other two, B2–O2 and B2–O3, with distances of 1.550(3) and 1.571(3) Å, respectively, fall in the range found for related carboxylate–BBN compounds,<sup>8i,12,13</sup> which suggest some covalent character. Again, the weak nature of the dative interactions in B1–O1 and B3–O4 may explain the higher symmetry observed in the  $^1\text{H}$  NMR spectra in solution. Assuming facile cleavage of these dative bonds in solution to form open structures, as well as formate–BBN intermolecular exchange reactions, fast on the NMR time scale, may average the two formate chemical environments, giving rise to a single resonance. We should note that two structures of formaldehyde–formate zwitterionic derivatives, both open-chain monomers, were reported by Wang and Stephan from the reaction of phosphines, H–BBN, and  $\text{CO}_2$ .<sup>8i</sup> However, the presence of an extra BBN unit in compound **1** allowed us to isolate and characterize not only the formaldehyde adduct **2** but also a formaldehyde–monoformate species with a polymeric structure (**3**) and, for the first time, a formaldehyde–bisformate compound with a macrocyclic structure (**4**). In the next section, kinetic experiments will shed more light on the role of these species in the catalytic hydroboration of  $\text{CO}_2$  with H–BBN.

#### Kinetic Studies for the Reduction of $\text{CO}_2$ with H–BBN.

A series of kinetic studies were carried out for the hydroboration of  $\text{CO}_2$  using diphenyl(vinyl)phosphine, **1**, and **2** as catalysts (1 mol %) at 25 and 60 °C. In these experiments, not only was formation of the reduction products, acetal **A** or methoxide **B**, monitored over time but also the

concentration of active species (Figures 4, 5, and S25–S28). The most outstanding feature in the experiments conducted at 25 °C was the presence of an induction period of ca. 4 h for the formation of **A** and **B** with catalysts  $\text{Ph}_2\text{PCHCH}_2$  and **1**. This period was absent for catalyst **2**, which accounts for the shorter reaction times observed (ca. 12 h) compared to the other two catalysts (18–20 h). Induction periods for the hydroboration of  $\text{CO}_2$  have been also detected with other catalysts such as phosphines (with H–BBN),<sup>8i</sup> phosphinoboronates (with  $\text{BH}_3$ ),<sup>8g</sup> and boryl amidinates (with H–BBN).<sup>8a</sup> In the latter two cases, these periods disappeared using the corresponding formaldehyde adducts as catalysts. We also followed the concentration of active species present in solution during catalysis at 25 °C with diphenyl(vinyl)phosphine and **1**. We noticed that the rapid increase of TON for the formation of products **A** and **B**, which took place after 4 h, coincided with the formation of compound **4**, which started to appear around the same time. In contrast, the only active species detected during the first 4 h were the adducts diphenyl(vinyl)phosphine–H–BBN (using  $\text{Ph}_2\text{PCHCH}_2$  as the catalyst) and **1**–HBBN (using **1** as the catalyst). In both cases, compound **2** started to appear at the late stages of the catalytic reaction, after ca. 14–15 h. By the end of the reaction, mixtures containing similar amounts of compounds **2** and **4** were obtained. In contrast, in catalysis with the formaldehyde adduct **2** at 25 °C, compound **4** was present from the beginning practically as the only active species during the first 1 h, when the activity was higher. After that period, the concentration of **4** dropped, and mixtures of **1**–HBBN, **2**, and **4** were obtained. These experiments revealed a correlation between the concentration of **4** and the activity of the catalysts. This was further confirmed after plotting instant turnover frequency (TOF) values for the formation of products  $[\text{d}(\text{TON A} + \text{B})/\text{d}t]$  versus time (Figure 5) because the highest TOF values were achieved when the concentration of **4** was highest. Kinetic studies performed at 60 °C for the mentioned catalysts showed much shorter induction periods when using compounds **1** and diphenyl(vinyl)phosphine (<5 min), whereas, once more, there was no induction period for the formaldehyde adduct **2**. Again, a correlation between the concentration of compound **4** and the activity of the catalyst was confirmed by the TOF versus time plots. However, compound **4** was a fleeting species in all cases at 60 °C, which lasted only a few minutes in solution at the beginning of the reaction, but its presence accounts for total TON values of up to 40 (i.e., 40% conversion to products) and instant TOF values ( $\text{A} + \text{B}$ ) of up to  $680 \text{ h}^{-1}$  (with catalyst **2**), roughly matching with the highest concentration of **4** in solution. After this time, compound **4** disappeared and only the adduct **1**–HBBN was detected. The activity dramatically decreased in all three instances up until the end of the monitored reaction (>90% conversion in all cases). All of these facts suggest an involvement of the bisformate derivative **4** in the reduction of  $\text{CO}_2$  with H–BBN.

Some valuable mechanistic information for the hydroboration of  $\text{CO}_2$  using phosphinoborane **1** as the catalyst could be gathered by combining the results from these kinetic studies and the stoichiometric reactions commented on before. In the first place, the adduct **1**–HBBN, generated in the presence of an excess of reactant H–BBN, will react with a molecule of  $\text{CO}_2$  like an intermolecular FLP to generate **Int-I** (Scheme 3), undetected in the reaction, which leads to free boron formate, also undetected. **Int-I** will react in the presence

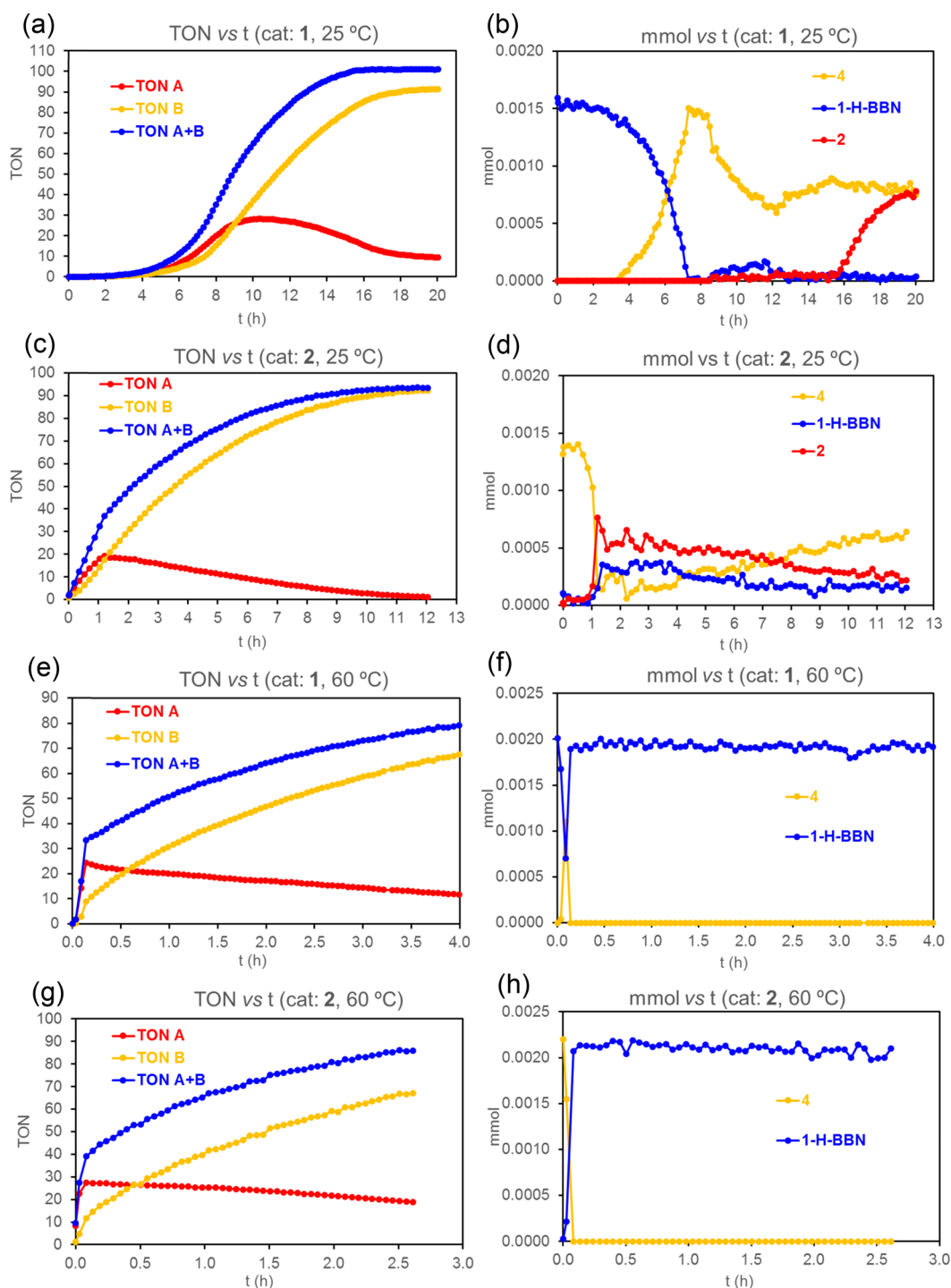


**Figure 4.** (a, c, e, and g) Total TON (A + B, blue ●), and TON for the formation of A (red ●) and CH<sub>3</sub>OBBN (B, yellow ●) versus time (h). (b, d, f, and h) Distribution of the active species 1-H-BBN (blue ●), 2 (red ●), and 4 (yellow ●) versus time for the reduction of CO<sub>2</sub> with H-BBN using catalysts 1 and 2 at 25 and 60 °C (1 mol % catalyst).

of more H-BBN to finally give compounds A (acetal) and B (methoxide) in a very slow fashion, hence the induction time detected. This reactivity resembles that proposed for the reduction of CO<sub>2</sub> with phosphines as catalysts.<sup>81</sup> Another possibility is that compound 1 will act as an intramolecular FLP, trapping a molecule of CO<sub>2</sub> to give zwitterionic intermediate **Int-II**. The reaction of **Int-II** with H-BBN will also generate free boron formate. In any event, the low activities displayed by 1 or 1-H-BBN, linked to the initial induction periods (ca. 4 h at room temperature), indicate that

these are not the main active species for the reduction of CO<sub>2</sub>. Indeed, the activity boost starts with the formation of macrocycle 4, which originates from compound 2, as we have already commented on. The formation of 2 can be explained by the reaction of acetal A (as a source of “free” formaldehyde) with compound 1, generating bisboranyl ether O(BBN)<sub>2</sub> as the byproduct. Once the formaldehyde adduct 2 is formed, an undetected open-chain intermediate must be obtained after cleavage of the O–B bond in the heterocycle and subsequent formation of a new one with an incoming H-

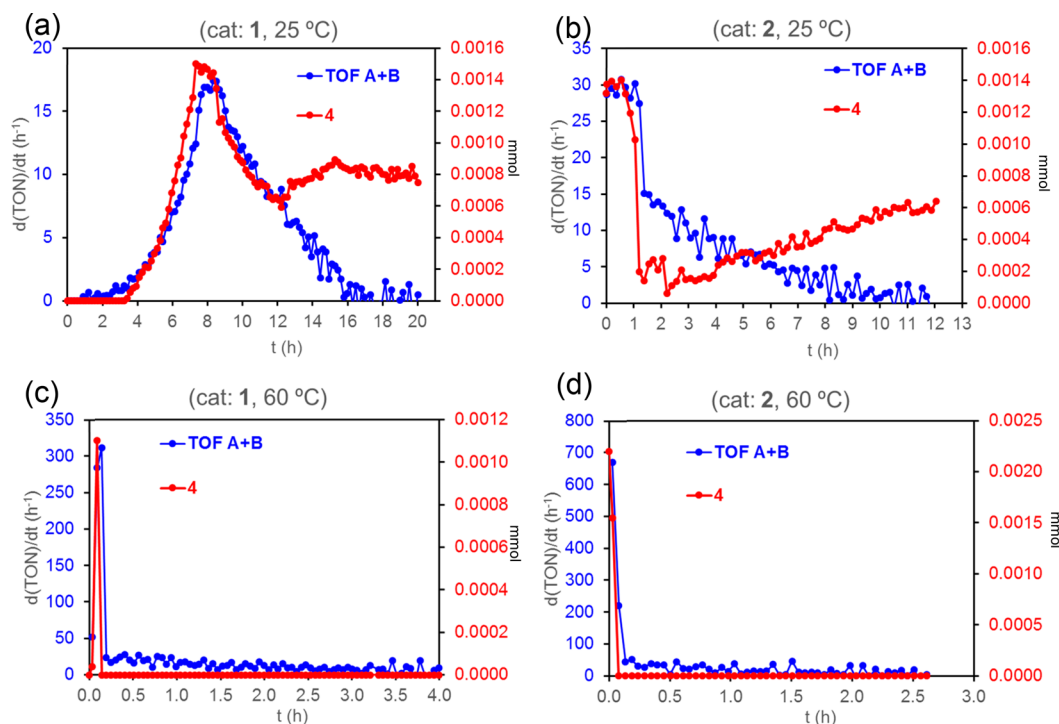
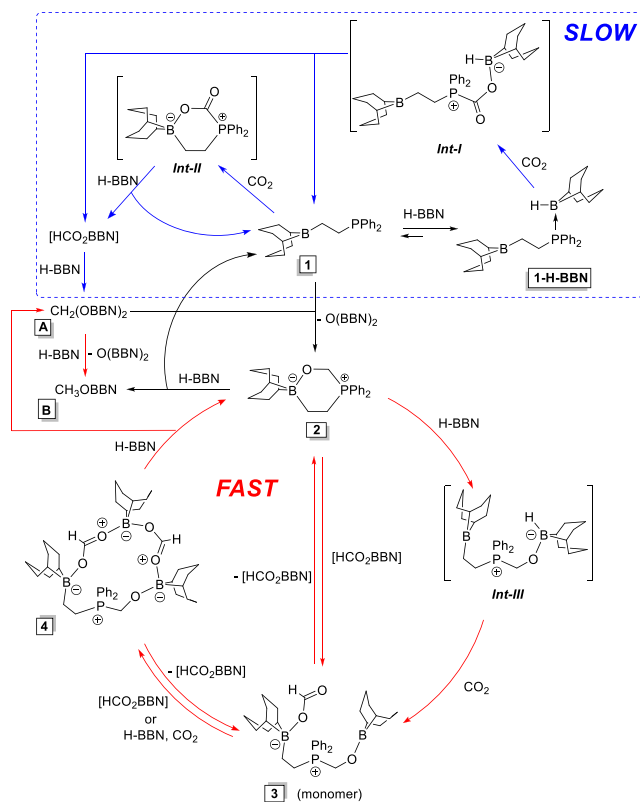


**Figure 5.** Plots comparing  $d(\text{TON A} + \text{B})/dt$  ( $\text{h}^{-1}$ ; blue ●) and millimoles of **4** (red ●) versus time (h) for the catalytic reduction of  $\text{CO}_2$  with H-BBN using catalysts **1** (a and c) and **2** (b and d) at 25 and 60 °C (1 mol % catalyst).

**Scheme 3. Proposed Mechanism for the Reduction of CO<sub>2</sub> with H-BBN Using Compound 1 as the Catalyst**



BBN molecule (**Int-III** in [Scheme 3](#)). A similar intermediate was computed for the hydroboration reaction of CO<sub>2</sub> using the formaldehyde adduct of a boron amidinate as the catalyst.<sup>8a</sup> Then, hydride attack of **Int-III** toward a CO<sub>2</sub> molecule will

give formate derivative **3** as a monomer. This reaction pathway for the generation of formate derivatives would be much faster than the previous ones (through **Int-I** and **Int-II**) because of the enhanced hydridic character of zwitterionic **Int-III**. In fact, it is known that borohydrides can react with CO<sub>2</sub>; Mizuta and co-workers proved that small amounts of NaBH<sub>4</sub> catalyze the reduction of CO<sub>2</sub> to the methanol level using BH<sub>3</sub> as the reductant,<sup>14</sup> whereas Cummins and co-workers showed that the stoichiometric reaction of NaBH<sub>4</sub> with 3 equiv of CO<sub>2</sub> generates the triformate compound Na[HB(OCHO)<sub>3</sub>].<sup>15</sup> Further reaction of **3** with more H-BBN and CO<sub>2</sub> will give bisformate **4**, detected during catalysis at both 25 and 60 °C. Because free HCO<sub>2</sub>BBN was not detected, we propose that adducts **3** and **4** “trap” formate molecules, enhancing their reactivity toward the second hydroboration reaction to give acetal **A** and regenerate the formaldehyde adduct **2**. Another possible pathway, as evidenced by NMR and the solid-state structures of **3** and **4**, would consist of fast equilibria between compounds **2**–**4** facilitated by fast boryl formate dissociation/coordination equilibria proposed for **3** and **4**. This would imply an active role for **2** as a catalyst for the hydroboration of boryl formate, directly leading to acetal **A** through equilibria with formate–formaldehyde species **3** and **4**. In this sense, Fontaine and co-workers calculated plausible formate adducts (undetected under experimental conditions) in fast equilibrium with the parent catalyst using *o*-(C<sub>6</sub>H<sub>4</sub>)(PPh<sub>2</sub>)(Bcat) in their mechanistic study of the hydroboration of CO<sub>2</sub> using HBcat.<sup>81</sup> In this reaction, the corresponding boryl formate was also undetected and assumed to react very fast with further equivalents of HBcat due to the action of the catalyst. One could assume that, in the early stages of the reaction with compound **2** as the catalyst, *p*(CO<sub>2</sub>) would still be high enough in the NMR tube so that CO<sub>2</sub> diffusion in the solution would not be the limiting step and the transformation of **2** into **4**, as well as the formation of acetal **A** and methoxide **B**, would



be fast. Alternatively, the presence of thermodynamically favored formate adduct **4** could be viewed as a consequence of the high activity of the formaldehyde adduct **2** as the active catalyst in the first and second hydroboration reactions. However, when the pressure of CO<sub>2</sub> drops and most of the borane is consumed at 60 °C, we conjectured that the formation of compound **4** would be less favored and the competing formaldehyde reduction reaction between **2** and H-BBN would be operative instead, giving methoxide **B** and compound **1**, which, in the presence of excess H-BBN, would be mainly in the form of adduct **1-H-BBN**. In contrast, the concentration of this adduct in the late stages of the reaction at 25 °C is almost negligible, meaning that the reduction of the formaldehyde unit of **2** is less favored at this temperature, and mixtures of **2** and **4** are obtained at these stages instead. In order to further verify the existence of this formaldehyde hydroboration reaction between **2** and H-BBN, NMR-scale kinetic experiments were carried out using <sup>13</sup>CO<sub>2</sub> and a higher catalyst load of compound **2** (2.5 mol %) to better monitor the formation of catalytic intermediates at 25 and 60 °C (Figures S29 and S30). In both experiments, we detected the formation of **B** in the <sup>1</sup>H NMR spectra, which can only be obtained by the direct reaction of H-BBN with the formaldehyde group of **2**, and <sup>13</sup>C isotopic enrichment in the active species **4**. Compound <sup>13</sup>C-**4** was identified by the presence of a doublet of doublets for the formaldehyde fragment in the region 4.5–5.0 ppm in the <sup>1</sup>H NMR spectra with a high <sup>1</sup>J<sub>CH</sub> coupling (ca. 149 Hz) and doublets at δ<sub>p</sub> ca. 26 ppm and δ<sub>C</sub> in the range 55–58 ppm in the <sup>31</sup>P and <sup>13</sup>C NMR spectra, respectively, with <sup>1</sup>J<sub>PC</sub> of ca. 70 Hz. However, the <sup>13</sup>C isotopic enrichment in the formaldehyde unit of **4** in the experiment at 25 °C was only ca. 30% after 14 h, whereas it was ca. 100% after 15 min at 60 °C, the time required to full conversion in both cases. This is in line with our previous results showing that direct hydroboration of the formaldehyde group of **2** takes place very slowly at 25 °C compared to the formation of acetal (**A**) or methoxide (**B**). It is worth noting that Fontaine and co-workers performed similar isotopic labeling experiments with different outcomes: using the formaldehyde adducts of phosphinoboronates *o*-C<sub>6</sub>H<sub>4</sub>(PR<sub>2</sub>)(Bcat) as catalysts, HBcat as the reductant, and <sup>13</sup>CO<sub>2</sub> at 70 °C, they did not find <sup>13</sup>C incorporation in the catalyst, meaning that the formaldehyde unit remained unscathed during catalysis.<sup>8g</sup>

**Catalytic Reduction of CO<sub>2</sub> with HBcat.** We also carried out the hydroboration of CO<sub>2</sub> using HBcat to give MeOBcat (**C**) with compounds **1** and **2** as catalysts at 60 °C (Table 2). We did not detect the presence of other reduction products in these reactions, such as formate or acetal derivatives, which is in line with the results reported by other authors using HBcat for the catalytic hydroboration of CO<sub>2</sub>.<sup>6,7,8g,h,l</sup> Ph<sub>2</sub>PCHCH<sub>2</sub> was also tested as the catalyst in a control experiment (entry 1). As can be seen, no reaction occurred at 60 °C for 14 h with 1 mol % catalyst load, which was not surprising regarding the lesser Lewis acidity of HBcat with respect to H-BBN. Thus, it seems evident from this experiment that (i) an intermolecular FLP between the phosphine and HBcat is not active for CO<sub>2</sub> hydroboration as opposed to the intramolecular FLP systems *o*-(C<sub>6</sub>H<sub>4</sub>)(PPh<sub>2</sub>)[B(OR)<sub>2</sub>] reported by Fontaine;<sup>7,8g,l</sup> (ii) direct hydroboration of the vinyl fragment of Ph<sub>2</sub>PCHCH<sub>2</sub> does not take place under the reaction conditions, as expected for less reactive dialkoxyboranes;<sup>16</sup> otherwise, we would expect the formation of an intramolecular FLP akin to that described by Fontaine that should be active in the hydroboration of CO<sub>2</sub>.

Table 2. Catalytic Hydroboration of CO<sub>2</sub> with HBcat<sup>a</sup>

$$\text{CO}_2 + \text{HBcat} \xrightarrow{\text{cat.}} \text{CH}_3\text{OBcat} + \text{O}(\text{Bcat})_2$$

**C**

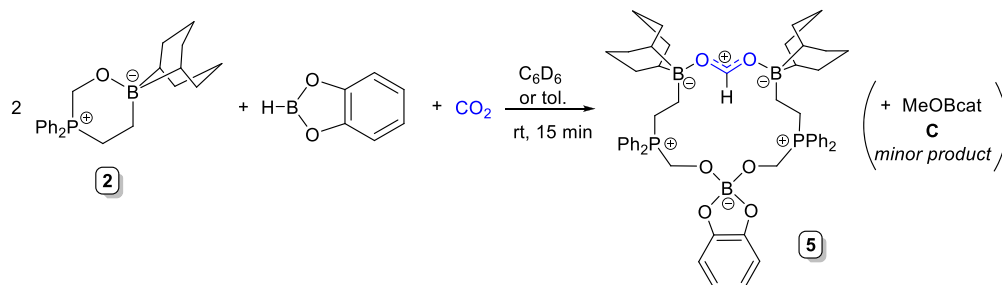
entry	catalyst	cat. load (mol %)	T (°C)	t (h)	conv (%) <sup>b</sup>	TON <sup>c</sup>
1	Ph <sub>2</sub> PCHCH <sub>2</sub>	1	60	14		
2	<b>1</b>	2.5	60	0.5	44	10.7
3	<b>1</b>	2.5	60	1	70	22.0
4	<b>1</b>	1	60	1		
5	<b>1</b>	1	60	15	90	73.2
6	<b>1</b>	0.1	60	9		
7	<b>2</b>	2.5	60	0.5	66	23.2
8	<b>2</b>	2.5	60	1	88	32.0
9	<b>2</b>	1	60	1	71	60.6
10	<b>2</b>	1	60	15	100	82.5
11	<b>2</b>	0.1	60	9		

<sup>a</sup>Reaction conditions: J. Young valve NMR tube containing ca. 0.6 mL C<sub>6</sub>D<sub>6</sub> solutions of HBcat (0.2 mmol), catalyst and internal standard [Si(SiMe<sub>3</sub>)<sub>4</sub>, 0.01 mmol], and CO<sub>2</sub> (1 atm). <sup>b</sup>Based on the relative integrals of HBcat and products in the <sup>11</sup>B NMR spectra. <sup>c</sup>Calculated according to the number of C–H bonds formed in the reduction products by integration of the corresponding signals relative to the internal standard in the <sup>1</sup>H NMR spectra.

As for compounds **1** and **2**, they turned out to be rather active for this transformation but less active than in the reductions with H-BBN, as indicated by the TON values, only up to 82.5 for compound **2** (1 mol %, entry 10) and 73.2 for compound **1** under the same conditions (entry 5). Moreover, catalyst loads down to 0.1 mol % were not tolerated (entries 6 and 11). The main difference observed between the catalytic activities of **1** and **2** was again related to the induction periods at early stages of the transformation. Thus, at a catalyst load of 1 mol %, there was no trace of the reduction product **C** after 1 h of using **1** as the catalyst (entry 4), whereas a TON of 60.6 was already measured with catalyst **2** at the same time (entry 9). This induction period disappeared with increasing catalyst load (2.5 mol %), although compound **2** was still slightly more active than **1**.

**Stoichiometric Reactions with HBcat and CO<sub>2</sub>.** During one of the catalytic runs with compound **2** as the catalyst (1 mol %), we detected only one P-containing species, displaying a sharp singlet ca. 24 ppm in the <sup>31</sup>P{<sup>1</sup>H} NMR spectrum, after 1 h at 60 °C. Signals in the <sup>1</sup>H NMR spectrum at ca. 8.6 and 4.8 ppm suggested another formaldehyde–formate derivative similar to **3** and **4**. However, after 15 h at the same temperature, a very broad signal was now observed in the <sup>31</sup>P{<sup>1</sup>H} NMR spectrum, also at ca. 24 ppm, and no downfield signals in the range expected for formate protons were present in the <sup>1</sup>H NMR but only a singlet at δ<sub>H</sub> 4.9 ppm attributed to a formaldehyde fragment. In an attempt to trap any of these intermediates, we first carried out the reaction between equimolar amounts of compound **2** and HBcat. Interestingly, a new species was identified, with a very broad signal in the <sup>31</sup>P{<sup>1</sup>H} NMR spectrum at ca. 17 ppm and a singlet in the <sup>1</sup>H NMR at 5.0 ppm ascribed to the formaldehyde fragment. This species is possibly an adduct involving interaction between the O atom of the formaldehyde group of **2** and the B center of the HBcat molecule. Unfortunately, this compound could be neither isolated nor crystallized for structural confirmation. However, Fontaine and co-workers also detected P-containing

Scheme 4. Preparation of Compound 5



species with resonances at  $\delta_p$  ca. 14 ppm in the reaction of the formaldehyde adduct of *o*-C<sub>6</sub>H<sub>4</sub>(P<sup>i</sup>Pr<sub>2</sub>)(Bcat) with HBcat in the absence of CO<sub>2</sub>.<sup>8g</sup> Although the mentioned species could not be isolated, they proposed it to be a Lewis adduct between one of the O atoms bound to B and HBcat, as well.

Additionally, we carried out the reaction of the formaldehyde adduct 2 and HBcat (1 equiv) under 1 atm of CO<sub>2</sub>, yielding a new macrocyclic derivative formulated as (HCO<sub>2</sub>)-{BBN(CH<sub>2</sub>)<sub>2</sub>(Ph<sub>2</sub>P)(CH<sub>2</sub>O)}<sub>2</sub>Bcat (5) and small amounts of methoxide C after only 15 min at room temperature (Scheme 4). Compound 5 crystallizes after a few hours under a CO<sub>2</sub> atmosphere from the reaction crude. The formation of 5 follows from the reaction of two molecules of 2 with one molecule of both HBcat and CO<sub>2</sub>. Interestingly, when we carried out the reaction with higher HBcat/2 ratios (up to 4:1) in the presence of CO<sub>2</sub>, compound 5 was still the only P-containing species detected, with increasing amounts of methoxide C as a side product. Some structural evidence for compound 5 was already found in the solution NMR spectra of reaction crudes: the relative integrals of the methylene protons of the two CH<sub>2</sub>O groups ( $\delta_H$  4.72 ppm) and that of the formate group ( $\delta_H$  8.79 ppm) in the <sup>1</sup>H NMR spectrum was 4:1, in agreement with the stoichiometry shown in Scheme 4. The latter groups also gave rise to signature signals in the <sup>13</sup>C NMR spectrum: a doublet at 56.0 ppm ( $J_{PC}$  = 72.1 Hz) and a singlet at 173.9 ppm, attributed to the formaldehyde groups and formate fragment, respectively. The chemically equivalent P atoms in 5 displayed a singlet in the <sup>31</sup>P{<sup>1</sup>H} NMR spectrum at 23.7 ppm, whereas two broad signals in the <sup>11</sup>B NMR spectrum at 19.4 (1B) and 10.8 (2B) ppm were assigned to the Bcat and two BBN fragments, respectively. To confirm that the formate group originated from the hydroboration of CO<sub>2</sub> with HBcat, an isotopic labeling experiment was carried out using <sup>13</sup>CO<sub>2</sub>, HBcat, and compound 2. In situ NMR characterization of the reaction mixture confirmed the presence of (<sup>13</sup>CHO<sub>2</sub>)-{BBN(CH<sub>2</sub>)<sub>2</sub>(Ph<sub>2</sub>P)(CH<sub>2</sub>O)}<sub>2</sub>Bcat (<sup>13</sup>C-5), with a diagnostic doublet in the <sup>1</sup>H NMR spectrum at 8.79 ppm with a <sup>1</sup>J<sub>CH</sub> of 207.2 Hz and a sharp singlet at 173.9 ppm for the isotopically enriched H<sup>13</sup>CO<sub>2</sub> group. We should note the small amounts of both <sup>12</sup>CH<sub>3</sub>OBcat (C) and <sup>13</sup>CH<sub>3</sub>OBcat (<sup>13</sup>C-C) were also detected in the <sup>1</sup>H NMR spectrum of the reaction crude. The unlabeled methoxide C must come from direct hydroboration of the formaldehyde fragment in 2. This reaction competes with the formation of 5, although it is less favored at room temperature. On the other hand, the isotopically enriched <sup>13</sup>C-C is a genuine byproduct of the hydroboration of <sup>13</sup>CO<sub>2</sub> mediated by compound 2. From all of the latter findings, we propose that formation of the macrocyclic compound 5 must be thermodynamically favored, even under an excess of borane, and is therefore the intermediate detected in the early stages of

the catalytic reduction of CO<sub>2</sub> with HBcat using catalyst 2. Mechanistically speaking, the formation of 5 would proceed via Lewis adduct formation between 2 and HBcat, detected previously in the stoichiometric reaction, which is presumably an open-chain species similar to Int-III in Scheme 3. The adduct 2-HBcat, in the presence of CO<sub>2</sub>, will give a formate derivative akin to monomer 3 in Scheme 3 with the formate on the BBN moiety. At this point, the formate-formaldehyde species would be trapped by another molecule of 2 to give 5, instead of reacting with more borane and CO<sub>2</sub> to give a compound similar to 4. This is likely due to the lesser Lewis acidity of HBcat compared to H-BBN.

Compound 5 was also detected in the sluggish reaction between compound 1, HBcat (2 equiv), and CO<sub>2</sub> at room temperature, together with considerable amounts of methoxide C (ratio of ca. 1:1 5/C). This indicates that a mechanism similar to that described for the reduction of CO<sub>2</sub> with H-BBN and 1 as the catalyst (vide supra) is also operative. Thus, the undetected formaldehyde adduct 2 must be initially formed in the reaction of phosphinoborane 1 and the acetal formed in the double hydroboration of CO<sub>2</sub> with HBcat [CH<sub>2</sub>(OBcat)<sub>2</sub>], which, in the presence of excess HBcat and CO<sub>2</sub>, gives rise to compound 5.

The structure of compound 5 was unambiguously confirmed by an X-ray diffraction study of a single crystal. This 16-membered zwitterionic macrocycle crystallized in the orthorhombic system *Pnma* (Figure 6). It consists of two molecules of the open-chain isomer of the formaldehyde adduct 2 after cleavage of the dative O → B bond, symmetrically trapping a formate unit (through two new O → B bonds between the O atoms of the formate and the BBN groups) and a Bcat moiety (through the O atoms of the formaldehyde units). The C<sub>2</sub> symmetry of this macrocycle is also evident in the asymmetric unit, as only half the molecule is present and the other half can be built up by C<sub>2</sub> rotation. Thus, there is symmetrical charge delocalization within the formate group, with C11–O2/O2' distances of 1.250(4) Å. The B–O distances between the Bcat fragment and formaldehyde groups, of 1.445(5) Å, are slightly shorter than that measured in the formaldehyde adduct *o*-C<sub>6</sub>H<sub>4</sub>(PPh<sub>2</sub>)(Bcat)(CH<sub>2</sub>O), of 1.473(3) Å,<sup>8l</sup> and consistent with covalent B–O bonds. In contrast, the B–O distances between the BBN fragments and formate group, of 1.612(3) Å, can be regarded as true dative O → B interactions (>1.6 Å).<sup>13</sup>

**Kinetic Studies for the Reduction of CO<sub>2</sub> with HBcat.** Kinetic studies were performed at 60 °C using compounds 1 and 2 as catalysts (1 mol %), following the formation of the methoxide product C (Figure 7). An induction period of ca. 1 h was clearly observed with catalyst 1, similar to that found in the reduction with H-BBN with the same catalyst. This was already evident in the catalytic runs commented on before (see

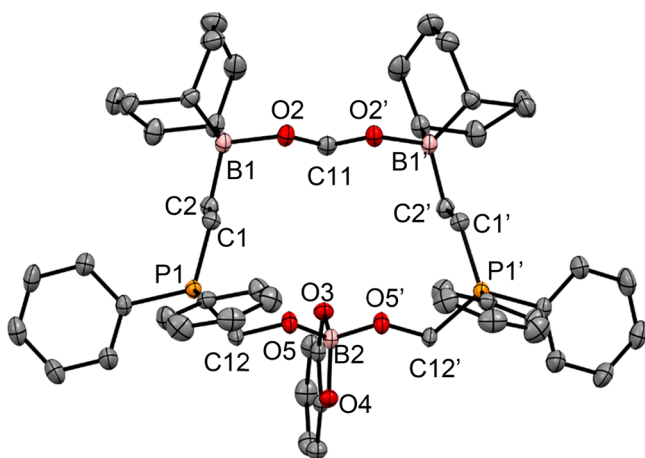


**Figure 6.** Molecular structure of compound **5**, with ellipsoids at the 30% probability level and H atoms and solvent molecules (toluene) omitted for clarity. Selected bond lengths (Å) and angles (deg): C2–B1 1.626(4), B1–O2 1.612(3), O2–C11 1.250(4), P1–C1 1.792(2), P1–C12 1.807(2), C12–O5 1.391(3), O5–B2 1.445(5), B2–O3 1.486(7), B2–O4 1.495(3); C2–B1–O2 104.4(2), O2–C11–O2' 121.4(6), C1–P1–C12 108.6(1), O5–B2–O5' 103.0(5).

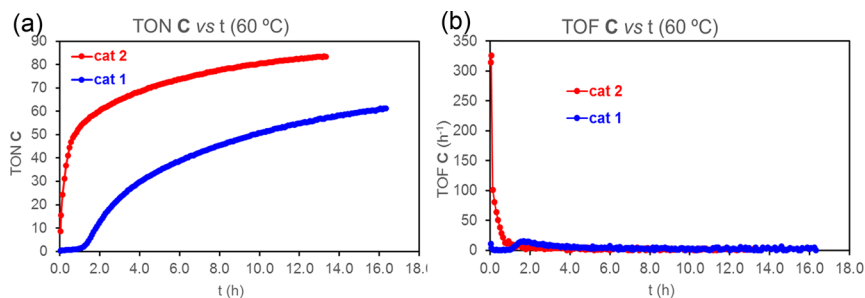
entry 4 in Table 2). After that time, there was a moderate activity boost to finally reach TON values of 61 after 16 h (ca. 70% conversion). Conversely, catalyst **2** was highly active from the beginning, already reaching a TON value of 50 in the first 45 min. The activity decayed significantly after the first 1 h to reach a TON of 83 after 13.3 h (ca. 90% conversion). In order to account for these results, we tried to monitor the concentrations of the intermediates and active species during catalysis. Pleasingly, we were able to establish a correlation again between the concentration of the bisformaldehyde–formate species **5** and the high initial TON (and TOF) values for catalysis with compound **2** (Figure S31c). In fact, total consumption of **5** occurred after 45 min at 60 °C, fitting nicely with the period of highest activity in the catalysis. Unfortunately, we were not able to identify other intermediates during the catalysis with **2**. As for catalyst **1**, we were not able to detect any of the intermediates identified in the stoichiometric studies, so the activity boost after 1 h could not be associated with compound **5** this time. We have previously established that the stoichiometric reaction of compound **1** with HBcat in the presence of CO<sub>2</sub> led to mixtures of compounds **2** and **5** at room temperature. It seems that the formation of compounds **2** and **5** is not favored under catalytic conditions at 60 °C, or the latter are too short-lived to be detected by NMR. This would also explain the lower TOF

values reached with catalyst **1** compared to those reached with **2** (maximum TOF values of 15 h<sup>−1</sup> for **1** vs 325 h<sup>−1</sup> for **2**; Figure 7b).

#### Catalytic Reduction of CO<sub>2</sub> with HBpin and BH<sub>3</sub>·SMe<sub>2</sub>.

HBpin was also used for the catalytic hydroboration of CO<sub>2</sub> with compounds **1** and **2** as catalysts (Table 3). Overall, the activity shown by these catalysts was lower than that with the other boranes because of the lesser reactivity of HBpin, as was already observed with other FLP-like P/B catalysts.<sup>7,8h</sup> In fact, much longer reaction times (days) were required to reach conversions of >85% under reaction conditions similar to those employed with previous hydroboranes (see, for example, entries 7 and 12). Moreover, mixtures of the mono-, di-, and trihydroboration products, HCO<sub>2</sub>Bpin (**D**), CH<sub>2</sub>(OBpin)<sub>2</sub> (**E**), and CH<sub>3</sub>OBpin (**F**), were obtained in most cases. This lack of selectivity in the reactions of HBcat with CO<sub>2</sub> was also observed not only with other metal-free P/B catalysts<sup>8h</sup> but also with transition-metal-based catalysts under certain conditions<sup>11a,c,12</sup> and is probably related to the lesser reactivity and higher steric hindrance of HBpin compared to HBcat, hampering the second and third hydroboration reactions. A control experiment with diphenyl(vinyl)phosphine (1 mol %) was also conducted (entry 1) and only trace amounts of formate **D** were detected after 14 h at 60 °C. Similar results in terms of activity and product distribution were obtained with catalysts **1** and **2** at 60 °C; i.e., conversions of 33 and 38% were achieved after 1 h at 60 °C employing 1 mol % catalyst load of **1** and **2**, respectively (entries 5 and 13). As expected, increasing catalyst load also increased conversion; for example, under the same reaction conditions as before but using 2.5 mol % catalyst loads of **1** and **2**, 62% conversion was obtained in both cases (entries 3 and 9). Likewise, increasing reaction time at 60 °C led to higher selectivity for the methoxide product **F** (entry 7). However, there are subtle changes in the activity of **1** and **2** at 25 °C, more specifically at short reaction times, because compound **1** only produced a trace amount of formate **D** (TON of 0.4 after ca. 20 min, entry 4), whereas compound **2** was much more active, also selectively generating formate **D** (TON value of 15.9 in ca. 10 min). This behavior is reminiscent of that found with the previous boranes, for which induction times were observed with catalyst **1** that were not present at all with **2**.

We tried to follow the formation of possible active species or resting states during the catalytic hydroboration of CO<sub>2</sub> with HBpin with catalysts **1** and **2**. In the first case, several peaks were observed in the <sup>31</sup>P NMR spectrum after 1 h at 60 °C, but only one, at δ<sub>p</sub> −11 ppm, remained after 48 h, which is probably ascribed to a resting state of the catalyst or a



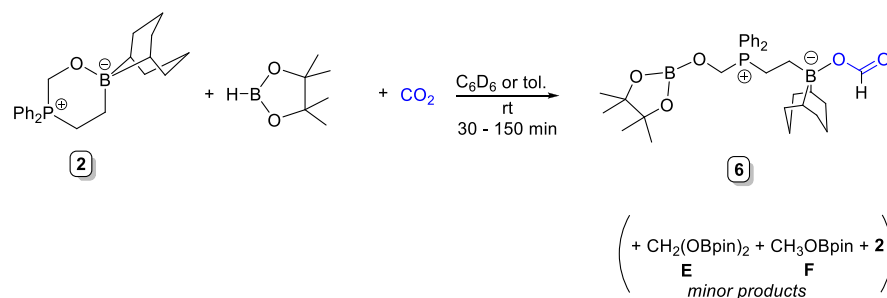
**Figure 7.** (a) TON for the formation of **C** versus time (h). (b) d(TON **C**)/dt (h<sup>−1</sup>) versus time (h) for the reduction of CO<sub>2</sub> with HBcat using catalyst **1** (blue ●) and catalyst **2** (red ●) (1 mol % catalyst).

Table 3. Catalytic Hydroboration of CO<sub>2</sub> with HBpin<sup>a</sup>

$$\text{CO}_2 + \text{HBpin} \xrightarrow{\text{cat.}} \underset{\text{D}}{\text{HCO}_2\text{Bpin}} + \underset{\text{E}}{\text{CH}_2(\text{OBpin})_2} + \underset{\text{F}}{\text{CH}_3\text{OBpin}} + \text{O(Bpin)}_2$$

entry	catalyst	cat. load (mol %)	T (°C)	t (h)	conv (%) <sup>b</sup>	TON <sup>c</sup> D	TON <sup>c</sup> E	TON <sup>c</sup> F
1	Ph <sub>2</sub> PCHCH <sub>2</sub>	1	60	14	3	1.5		
2	1	2.5	60	0.5	45	9.2	4.3	4.2
3	1	2.5	60	1	62	7.9	7.4	7.4
4	1	1	25	0.3	<1	0.4		
5	1	1	60	1	33	10.9	10.1	8.9
6	1	1	60	5	60	4.1	33.0	21.9
7	1	1	60	48	94		3.7	88.2
8	2	2.5	60	0.5	50	4.7	5.7	8.3
9	2	2.5	60	1	62	5.6	7.8	9.5
10	2	1	25	0.2	23	15.9		
11	2	1	25	2	41	27.3	2.4	
12	2	1	25	96	87	7.2	13.3	49.0
13	2	1	60	1	38	11.4	10.4	10.6
14	2	1	60	15	71		26.2	42.3

<sup>a</sup>Reaction conditions: J. Young valve NMR tube containing ca. 0.6 mL C<sub>6</sub>D<sub>6</sub> solutions of HBpin (0.2 mmol), catalyst and internal standard [Si(SiMe<sub>3</sub>)<sub>4</sub>, 0.01 mmol], and CO<sub>2</sub> (1 atm). <sup>b</sup>Based on the relative integrals of HBcat and products in the <sup>11</sup>B NMR spectra. <sup>c</sup>Calculated according to the number of C–H formed in the reduction products by integration of the corresponding signals relative to the internal standard.

Scheme 5. Stoichiometric Reaction between 2, HBcat, and CO<sub>2</sub>Table 4. Catalytic Hydroboration of CO<sub>2</sub> with BH<sub>3</sub>·SMe<sub>2</sub><sup>a</sup>

$$\text{CO}_2 + \text{BH}_3\cdot\text{SMe}_2 \xrightarrow{\text{cat.}} \underset{\text{G}}{\text{MeO-B-O-B-OMe}} + \underset{\text{H}}{\text{B(OMe)}_3}$$

entry	catalyst	cat. load (mol %)	T (°C)	t (h)	conv (%) <sup>b</sup>	TON <sup>c</sup> G	TON <sup>c</sup> H
1	Ph <sub>2</sub> PCHCH <sub>2</sub>	2	25	14			
2	1	1	60	14	3	7.7	
3	2	1	25	1	62	161.0	15.8
4	2	1	60	0.2	65	201.2	17.5
5	2	1	60	0.5	86	254.0	21.0
6	2	1	60	1	95	285.8	22.0
7	2	0.1	60	1	13	373.0	20.0

<sup>a</sup>Reaction conditions: J. Young valve Schlenk flask with a stir bar, containing ca. 0.8 mL C<sub>6</sub>D<sub>6</sub> solutions of BH<sub>3</sub>·SMe<sub>2</sub> (0.5 mmol), catalyst and internal standard [Si(SiMe<sub>3</sub>)<sub>4</sub>, 0.01 mmol], and CO<sub>2</sub> (1 atm). <sup>b</sup>Based on the relative integrals of BH<sub>3</sub>·SMe<sub>2</sub> and products in the <sup>11</sup>B NMR. <sup>c</sup>Calculated according to the number of C–H bonds formed in the reduction products by integration of the corresponding signals relative to the internal standard.

deactivated species. The nature of this species could not be ascertained because it was not detected in subsequent stoichiometric reactions. In contrast, a single peak was detected in the <sup>31</sup>P NMR spectrum, at δ<sub>p</sub> 26 ppm after 0.2 h at 25 °C using catalyst 2. When we carried out the stoichiometric reaction between equimolar amounts of HBpin and compound 2, in the presence of CO<sub>2</sub> (1 atm), we obtained, after a few

minutes, a major product with a signature singlet at δ<sub>p</sub> 26 ppm in the <sup>31</sup>P NMR spectrum that we formulate as the formate–formaldehyde compound (HCO<sub>2</sub>)BBN(CH<sub>2</sub>)<sub>2</sub>(Ph<sub>2</sub>P)–(CH<sub>2</sub>O)Bpin (6) and small amounts of acetal E, methoxide F, and unreacted 2 (Scheme 5). The match in the <sup>31</sup>P NMR spectrum between compound 6 and the species detected in the reaction with catalyst 2 at 25 °C led us to assume that both are



the same species. However, compound **6** turned out to be less stable than its BBN or Bcat counterparts **3–5** because small amounts of **2** were always present in the NMR spectra even after workup attempting to isolate it as a pure species. Crystals of **6** suitable for a diffractometric analysis could not be obtained either, but the NMR data collected allowed us to confidently confirm the monoformate–monoformaldehyde nature of this compound. Thus, the integral ratio between the formate proton [ $\delta_{\text{H}}$  8.95 ppm ( $\text{C}_6\text{D}_6$ ) or 8.32 ppm ( $\text{CD}_2\text{Cl}_2$ )] and the methylene protons of the formaldehyde [ $\delta_{\text{H}}$  4.99 ppm ( $\text{C}_6\text{D}_6$ ) or 5.11 ppm ( $\text{CD}_2\text{Cl}_2$ )] was roughly 1:2, in good agreement with the proposed structure. The rest of the NMR data were also in line with our proposal, with the most outstanding features being two broad signals observed in the  $^{11}\text{B}$  NMR spectrum, at  $\delta_{\text{B}}$  22.3 and 1.9 ppm, in the expected regions for a tricoordinate borate ester (OBpin) and a tetracoordinate borate ( $\text{CH}_2$ )(O)BBN fragment. Thus, it seems that the higher steric demands of the Bpin group probably preclude further reaction with another molecule of **2** to give a macrocycle akin to **5**.

Finally, we also tested  $\text{BH}_3\cdot\text{SMe}_2$  for the catalytic hydroboration of  $\text{CO}_2$  with catalysts **1** and **2**. As commented on in the Introduction, Fontaine and co-workers used this reductant for the first time for this type of reaction,<sup>7</sup> employing phosphinoboronates as catalysts, with excellent results in terms of activity. Because initial tests at NMR scale showed poor conversions, we decided to use Schlenk flasks equipped with J. Young stoppers instead to make sure  $\text{CO}_2$  was not the limiting reagent. First, the control experiment with diphenyl(vinyl)phosphine showed negligible activity at 25 °C for 14 h (entry 1, Table 4). Likewise, catalyst **1** turned out to be almost inactive even at 60 °C (entry 2). This is not at all surprising because two of the phosphinoboronates of the formula  $o\text{-(C}_6\text{H}_4\text{)}(\text{PPh}_2)[\text{B}(\text{OR})_2]$  reported by Fontaine also showed little to no activity in the catalytic reduction of  $\text{CO}_2$  with  $\text{BH}_3$ .<sup>8g</sup> In contrast, the formaldehyde adduct **2** proved to be very active for this transformation to yield mixtures of methoxide products [ $(\text{OMeBO})_3$  (**G**, major product) and  $\text{B}(\text{OMe})_3$  (**H**, minor product; entries 3–7). As expected, increasing temperature led to higher activities, rising conversions from 62% at 25 °C to 95% at 60 °C after 1 h with a catalyst load of 1 mol % (entries 3 and 6). Higher activities, in terms of TOF values, were measured at shorter reaction times. Thus, total TON values of 218.7 and 305.8 were calculated after 0.2 and 1 h at 60 °C, respectively (average TOF values of 1093.5 and 305.8  $\text{h}^{-1}$ , entries 4 and 6). Catalyst loads down to 0.1 mol % were tolerated, keeping the same concentration of borane but with lower conversions (13%) and total TON values of 393 after 1 h at 60 °C (entry 7).

In our case, not only was the formaldehyde adduct **2** a very active catalyst for the reduction of  $\text{CO}_2$  with  $\text{BH}_3$ , but also the phosphinoborane **1** turned out to be essentially inactive under the same conditions, ruling out an FLP-type mechanism in which the  $\text{CO}_2$  molecule is trapped by the phosphinoborane and the borane reduces the activated  $\text{CO}_2$  molecule. After analyzing the NMR spectra at the end of the catalytic run in entry 6, we noticed a major P-containing species in the  $^{31}\text{P}$  NMR spectrum, displaying a broad signal at  $\delta_{\text{P}}$  19.3 ppm, attributed to the Lewis adduct between phosphinoborane **1** and  $\text{BH}_3$  (**1-BH<sub>3</sub>**). In order to confirm this hypothesis, we conducted the reaction between compound **1** and  $\text{BH}_3\cdot\text{SMe}_2$  to obtain the expected adduct,  $(\text{BH}_3)\text{Ph}_2\text{P}(\text{CH}_2)_2\text{BBN}$  (**1-BH<sub>3</sub>**), in high yields. The NMR spectra of **1-BH<sub>3</sub>** are in good

agreement with the structural proposal for this adduct. One of the most diagnostic signals of this species was a very broad resonance in the range 2.2–1.3 ppm in the  $^1\text{H}$  NMR spectrum, assigned to the  $\text{BH}_3$  unit, which became a sharp singlet at  $\delta_{\text{H}}$  1.83 ppm in a  $^1\text{H}\{^{11}\text{B}\}$  NMR experiment. A broad multiplet due to  $^1J(^{31}\text{P}-^{11}\text{B})$  was also observed at  $\delta_{\text{P}}$  19.3 ppm in the  $^{31}\text{P}\{^1\text{H}\}$  NMR spectrum, matching with that observed in the catalytic reaction. The  $^{11}\text{B}$  and  $^{11}\text{B}\{^1\text{H}\}$  NMR spectra were also very informative, displaying both a broad downfield signal at  $\delta_{\text{B}}$  ca. 85 ppm, in the region expected for a tricoordinate boron of a  $\text{CH}_2\text{BBN}$  fragment, and an upfield quadruplet of doublets ( $^{11}\text{B}$ ) at  $\delta_{\text{B}}$  –38.6 ppm for the tetracoordinate boron of the  $\text{BH}_3$  moiety, which turned into a doublet in the  $^1\text{H}$ -decoupled experiment ( $^1J_{\text{BP}} = 57$  Hz). The latter signals were also detected as low-intensity resonances in the  $^{11}\text{B}$  NMR spectrum of the catalytic experiment.

We also carried out other stoichiometric experiments in an attempt to trap or detect intermediates relevant to the catalytic reduction of  $\text{CO}_2$  with  $\text{BH}_3$ . In the first place, the reaction of compound **2** (0.07 mmol) with  $\text{BH}_3\cdot\text{SMe}_2$  (0.10 mmol) in the presence of  $\text{CO}_2$  was conducted in an NMR tube. The NMR spectra recorded immediately after exposure to a  $\text{CO}_2$  atmosphere showed complete conversion of the borane to reduction products **G** and **H** in a 2:1 ratio, as well as a mixture of compounds **2** and **1-BH<sub>3</sub>**, which obviously follows from reaction of the formaldehyde group with  $\text{BH}_3$  to give **1** and subsequent formation of a Lewis adduct between **1** and another molecule of  $\text{BH}_3$ . Because we were not able to detect other intermediates, we decided to monitor the reaction between **2** and  $\text{BH}_3\cdot\text{SMe}_2$  in the absence of  $\text{CO}_2$ . We noticed that complete reduction of the formaldehyde unit in **2** to give **1-BH<sub>3</sub>** takes ca. 3 h, generating small amounts of reduction products, **G** and **H**, but in an inverse ratio, 1:2, together with unreacted borane. At short reaction times (10 min), we were able to detect a plausible Lewis adduct between **2** and  $\text{BH}_3$ , most likely by interaction between the O atom in **2** and the B center of  $\text{BH}_3$ . Some diagnostic resonances support this formulation, such as a singlet at 4.75 ppm in the  $^1\text{H}$  NMR spectrum, ascribed to the methylene protons of the  $\text{CH}_2\text{O}$  unit or a multiplet in the  $^{31}\text{P}\{^1\text{H}\}$  NMR spectrum at 24.1 ppm, resembling that found for **1-BH<sub>3</sub>**, suggesting  $^{31}\text{P}-^{11}\text{B}$  coupling. Moreover, this adduct was the major P-containing species after 10 min, with small amounts of **2** and **1-BH<sub>3</sub>**. Finally, we also carried out the reaction between **1**,  $\text{BH}_3\cdot\text{SMe}_2$  (molar ratio 1:3), and  $\text{CO}_2$ . As expected, the formation of methanol-level products **G** and **H** was practically negligible after 1 h at room temperature, in stark contrast to the experiment with compound **2**. However, after that time, reduction products started to form sluggishly, yielding a mixture of **G** and **H** in a 10:1 ratio after 22 h. The only P-containing species detected throughout the reaction was adduct **1-BH<sub>3</sub>**. From all of these stoichiometric experiments, we can deduce that **1-BH<sub>3</sub>** is not completely inactive for the catalytic reduction of  $\text{CO}_2$  with  $\text{BH}_3$  but is much less active than compound **2**. We also observed that, once more, reduction of the formaldehyde unit in **2** was a competitive reaction in this transformation, which transformed **2** into the almost inactive **1-BH<sub>3</sub>**, detected as the resting state of the catalyst at the end of the catalysis. A plausible Lewis adduct formed between **2** and  $\text{BH}_3$  was detected as an intermediate in the stoichiometric reactions conducted but not isolated because of its fleeting existence in solution.

## CONCLUSIONS

Overall, in this paper we have proven that the formaldehyde adduct of phosphinoborane **1** and its formaldehyde–formate derivatives play an essential role in the catalytic hydroboration of CO<sub>2</sub> with four different hydroboranes, using **1** as the catalyst. Thus, the a priori more obvious intramolecular FLP pathway for the direct reduction of a CO<sub>2</sub> molecule once trapped by the phosphinoborane turns out to be a less active route. This usually leads to induction periods that can last for hours at room temperature, the time required for the sluggish formation of enough amounts of acetal, the source of free formaldehyde, to react with phosphinoborane to give the formaldehyde adduct **2**. In fact, the main operative pathway for the catalytic hydroboration of CO<sub>2</sub> involves this adduct, which forms formaldehyde–hydroborane intermediates, detected in some instances but not isolated in this work. The enhanced hydridic character of these adducts enables the first hydroboration of CO<sub>2</sub> to boryl formate, which always requires a catalyst. Free boryl formate, undetected in reactions with H-BBN and HBcat, is readily trapped by the formaldehyde adduct to form formaldehyde–formate derivatives, some of them fully characterized for the first time in this work, which mediate in the hydroboration of boryl formate to bisboryl acetal. Deactivation pathways often involve reduction of the formaldehyde moiety in the late stages of the catalysis when most of the borane and/or CO<sub>2</sub> have been consumed, thus regenerating the nearly inactive phosphinoborane catalyst.

In terms of the catalyst activity (TON and TOF values measured per the number of C–H bonds formed in the products) with different secondary boranes tested under the same reaction conditions (NMR scale), the order goes as follows: H-BBN > HBcat > HBpin. This is indeed the expected order, taking into account the reactivity of the boranes themselves. The only differences observed using phosphinoborane or its formaldehyde adduct as the catalyst with these boranes are the induction periods at the beginning of the reactions, detected for the former, thus reducing the activity in the early stages of the catalysis. In terms of selectivity, the methoxide derivative is the only product detected in the catalysis with HBcat, probably because of the lesser steric demands of this borane, whereas mixtures of acetal and methoxide are obtained for H-BBN. Reductions with the less active and bulky HBpin often lead to mixtures of the three products (formate, acetal, and methoxide), but at short reaction times, the formate can be obtained almost selectively with the formaldehyde adduct as the catalyst. BH<sub>3</sub>·SMe<sub>2</sub>, tested under different conditions (Schlenk scale), shows an activity comparable to that of H-BBN but only when the formaldehyde adduct is used as the catalyst because the phosphinoborane **1** shows almost negligible activity. A mixture of two methoxide-level products is always obtained with this active borane.

## ASSOCIATED CONTENT

### Supporting Information

The Supporting Information is available free of charge at <https://pubs.acs.org/doi/10.1021/acs.inorgchem.0c01152>.

General remarks, synthetic protocols, and NMR spectra for new compounds and stoichiometric reactions, general protocols and NMR spectra for the catalytic reduction of CO<sub>2</sub> with hydroboranes, kinetic experiments, and X-ray crystal determination (PDF)

## Accession Codes

CCDC 1995178–1995181 contain the supplementary crystallographic data for this paper. These data can be obtained free of charge via [www.ccdc.cam.ac.uk/data\\_request/cif](http://www.ccdc.cam.ac.uk/data_request/cif), or by emailing [data\\_request@ccdc.cam.ac.uk](mailto:data_request@ccdc.cam.ac.uk), or by contacting The Cambridge Crystallographic Data Centre, 12 Union Road, Cambridge CB2 1EZ, UK; fax: +44 1223 336033.

## AUTHOR INFORMATION

### Corresponding Author

Alberto Ramos – Departamento de Química Inorgánica, Orgánica y Bioquímica, Centro de Innovación en Química Avanzada (ORFEO-CINQA), Universidad de Castilla–La Mancha, E-13071 Ciudad Real, Spain; [orcid.org/0000-0001-7993-7864](https://orcid.org/0000-0001-7993-7864); Email: [Alberto.Ramos@uclm.es](mailto:Alberto.Ramos@uclm.es)

### Authors

Antonio Antiñolo – Departamento de Química Inorgánica, Orgánica y Bioquímica, Centro de Innovación en Química Avanzada (ORFEO-CINQA), Universidad de Castilla–La Mancha, E-13071 Ciudad Real, Spain; [orcid.org/0000-0002-4417-6417](https://orcid.org/0000-0002-4417-6417)

Fernando Carrillo-Hermosilla – Departamento de Química Inorgánica, Orgánica y Bioquímica, Centro de Innovación en Química Avanzada (ORFEO-CINQA), Universidad de Castilla–La Mancha, E-13071 Ciudad Real, Spain; [orcid.org/0000-0002-1187-7719](https://orcid.org/0000-0002-1187-7719)

Rafael Fernández-Galán – Departamento de Química Inorgánica, Orgánica y Bioquímica, Centro de Innovación en Química Avanzada (ORFEO-CINQA), Universidad de Castilla–La Mancha, E-13071 Ciudad Real, Spain; [orcid.org/0000-0001-5832-6247](https://orcid.org/0000-0001-5832-6247)

Complete contact information is available at: <https://pubs.acs.org/doi/10.1021/acs.inorgchem.0c01152>

### Author Contributions

The manuscript was written through contributions of all authors. All authors have given approval to the final version of the manuscript.

### Notes

The authors declare no competing financial interest.

## ACKNOWLEDGMENTS

We gratefully acknowledge financial support from the Ministerio de Economía y Competitividad (MINECO), Spain (Grants CTQ2016-77614-P and CTQ2016-81797-REDC). We also thank Dr. D. Elorriaga for invaluable assistance in X-ray structure analysis. A.R. acknowledges a postdoctoral contract funded by the “Plan Propio de I + D + i” of the Universidad de Castilla–La Mancha.

## REFERENCES

- (1) Aresta, M. *Carbon Dioxide as Chemical Feedstock*; Wiley-VCH Verlag GmbH & Co. KGaA, 2010; p 394.
- (2) (a) Olah, G. A.; Goeppert, A.; Prakash, G. K. S. *Beyond Oil and Gas: The Methanol Economy*; Wiley-VCH Verlag GmbH & Co. KGaA, 2009; p 334. (b) Olah, G. A.; Goeppert, A.; Prakash, G. K. S. Chemical Recycling of Carbon Dioxide to Methanol and Dimethyl Ether: From Greenhouse Gas to Renewable, Environmentally Carbon Neutral Fuels and Synthetic Hydrocarbons. *J. Org. Chem.* **2009**, *74*, 487–498.
- (3) (a) Sordakis, K.; Tang, C.; Vogt, L. K.; Junge, H.; Dyson, P. J.; Beller, M.; Laurenczy, G. Homogeneous Catalysis for Sustainable

Hydrogen Storage in Formic Acid and Alcohols. *Chem. Rev.* **2018**, *118*, 372–433. (b) Kar, S.; Kothandaraman, J.; Goepfert, A.; Prakash, G. K. S. Advances in catalytic homogeneous hydrogenation of carbon dioxide to methanol. *J. CO<sub>2</sub> Util.* **2018**, *23*, 212–218. (c) Dong, K.; Razaq, R.; Hu, Y.; Ding, K. Homogeneous Reduction of Carbon Dioxide with Hydrogen. *Top. Curr. Chem.* **2017**, *375*, 23. (d) Bernskoetter, W. H.; Hazari, N. Reversible Hydrogenation of Carbon Dioxide to Formic Acid and Methanol: Lewis Acid Enhancement of Base Metal Catalysts. *Acc. Chem. Res.* **2017**, *50*, 1049–1058. (e) Klankermayer, J.; Wesselbaum, S.; Beydoun, K.; Leitner, W. Selective Catalytic Synthesis Using the Combination of Carbon Dioxide and Hydrogen: Catalytic Chess at the Interface of Energy and Chemistry. *Angew. Chem., Int. Ed.* **2016**, *55*, 7296–7343. (f) Wang, W.-H.; Himeda, Y.; Muckerman, J. T.; Manbeck, G. F.; Fujita, E. CO<sub>2</sub> Hydrogenation to Formate and Methanol as an Alternative to Photo- and Electrochemical CO<sub>2</sub> Reduction. *Chem. Rev.* **2015**, *115*, 12936–12973. (g) Alberico, E.; Nielsen, M. Towards a methanol economy based on homogeneous catalysis: methanol to H<sub>2</sub> and CO<sub>2</sub> to methanol. *Chem. Commun.* **2015**, *51*, 6714–6725.

(4) (a) Wang, X.; Xia, C.; Wu, L. Homogeneous carbon dioxide reduction with p-block element-containing reductants. *Green Chem.* **2018**, *20*, 5415–5426. (b) Fontaine, F. G.; Rochette, E. Ambiphilic Molecules: From Organometallic Curiosity to Metal-Free Catalysts. *Acc. Chem. Res.* **2018**, *51*, 454–464. (c) Dagorne, S.; Wehmschulte, R. Recent Developments on the Use of Group 13 Metal Complexes in Catalysis. *ChemCatChem* **2018**, *10*, 2509–2520. (d) Fontaine, F.-G.; Stephan, D. W. Metal-free reduction of CO<sub>2</sub>. *Curr. Opin. Green Sustain. Chem.* **2017**, *3*, 28–32. (e) Fontaine, F.-G.; Courtemanche, M.-A.; Légaré, M.-A.; Rochette, E. Design principles in frustrated Lewis pair catalysis for the functionalization of carbon dioxide and heterocycles. *Coord. Chem. Rev.* **2017**, *334*, 124–135. (f) Bontemps, S. Boron-mediated activation of carbon dioxide. *Coord. Chem. Rev.* **2016**, *308*, 117–130. (g) Chong, C. C.; Kinjo, R. Catalytic Hydroboration of Carbonyl Derivatives, Imines, and Carbon Dioxide. *ACS Catal.* **2015**, *5*, 3238–3259. (h) Chakraborty, S.; Bhattacharya, P.; Dai, H.; Guan, H. Nickel and iron pincer complexes as catalysts for the reduction of carbonyl compounds. *Acc. Chem. Res.* **2015**, *48*, 1995–2003. (i) Fontaine, F.-G.; Courtemanche, M.-A.; Légaré, M.-A. Transition-metal-free catalytic reduction of carbon dioxide. *Chem. - Eur. J.* **2014**, *20*, 2990–2996.

(5) Fernández-Alvarez, F. J.; Aitani, A. M.; Oro, L. A. Homogeneous catalytic reduction of CO<sub>2</sub> with hydrosilanes. *Catal. Sci. Technol.* **2014**, *4*, 611–624.

(6) Chakraborty, S.; Zhang, J.; Krause, J. A.; Guan, H. An Efficient Nickel Catalyst for the Reduction of Carbon Dioxide with a Borane. *J. Am. Chem. Soc.* **2010**, *132*, 8872–8873.

(7) Courtemanche, M.-A.; Légaré, M.-A.; Maron, L.; Fontaine, F.-G. A highly active phosphine-borane organocatalyst for the reduction of CO<sub>2</sub> to methanol using hydroboranes. *J. Am. Chem. Soc.* **2013**, *135*, 9326–9329.

(8) (a) Ramos, A.; Antiñolo, A.; Carrillo-Hermosilla, F.; Fernández-Galán, R.; Rodríguez-Diéguez, A.; García-Vivó, D. Carbodiimides as catalysts for the reduction of CO<sub>2</sub> with boranes. *Chem. Commun.* **2018**, *54*, 4700–4703. (b) Yang, Y.; Yan, L.; Xie, Q.; Liang, Q.; Song, D. Zwitterionic indenylammonium with carbon-centred reactivity towards reversible CO<sub>2</sub> binding and catalytic reduction. *Org. Biomol. Chem.* **2017**, *15*, 2240–2245. (c) von Wolff, N.; Lefevre, G.; Berthet, J. C.; Thuéry, P.; Cantat, T. Implications of CO<sub>2</sub> Activation by Frustrated Lewis Pairs in the Catalytic Hydroboration of CO<sub>2</sub>: A View Using N/Si<sup>+</sup> Frustrated Lewis Pairs. *ACS Catal.* **2016**, *6*, 4526–4535. (d) Sau, S. C.; Bhattacharjee, R.; Vardhanapu, P. K.; Vijaykumar, G.; Datta, A.; Mandal, S. K. Metal-Free Reduction of CO<sub>2</sub> to Methoxyborane under Ambient Conditions through Borondifluoride Formation. *Angew. Chem., Int. Ed.* **2016**, *55*, 15147–15151. (e) Yang, Y.; Xu, M.; Song, D. Organocatalysts with carbon-centered activity for CO<sub>2</sub> reduction with boranes. *Chem. Commun.* **2015**, *51*, 11293–11296. (f) Ho, S. Y. F.; So, C.-W.; Saffon-Merceron, N.; Mézailles, N. Formation of a zwitterionic boronium species from the reaction of a stable carbenoid with borane: CO<sub>2</sub> reduction. *Chem. Commun.* **2015**,

*51*, 2107–2110. (g) Declercq, R.; Bouhadir, G.; Bourissou, D.; Légaré, M.-A.; Courtemanche, M.-A.; Nahí, K. S.; Bouchard, N.; Fontaine, F.-G.; Maron, L. Hydroboration of Carbon Dioxide Using Ambiphilic Phosphine–Borane Catalysts: On the Role of the Formaldehyde Adduct. *ACS Catal.* **2015**, *5*, 2513–2520. (h) Wang, T.; Stephan, D. W. Carbene-9-BBN ring expansions as a route to intramolecular frustrated Lewis pairs for CO<sub>2</sub> reduction. *Chem. - Eur. J.* **2014**, *20*, 3036–3039. (i) Wang, T.; Stephan, D. W. Phosphine catalyzed reduction of CO<sub>2</sub> with boranes. *Chem. Commun.* **2014**, *50*, 7007–7010. (j) Légaré, M.-A.; Courtemanche, M.-A.; Fontaine, F.-G. Lewis base activation of borane-dimethylsulfide into strongly reducing ion pairs for the transformation of carbon dioxide to methoxyboranes. *Chem. Commun.* **2014**, *50*, 11362–11365. (k) Das Neves Gomes, C.; Blondiaux, E.; Thuéry, P.; Cantat, T. Metal-free reduction of CO<sub>2</sub> with hydroboranes: two efficient pathways at play for the reduction of CO<sub>2</sub> to methanol. *Chem. - Eur. J.* **2014**, *20*, 7098–7106. (l) Courtemanche, M.-A.; Légaré, M.-A.; Maron, L.; Fontaine, F.-G. Reducing CO<sub>2</sub> to methanol using frustrated Lewis pairs: on the mechanism of phosphine-borane-mediated hydroboration of CO<sub>2</sub>. *J. Am. Chem. Soc.* **2014**, *136*, 10708–10717. (m) Sokolovicz, Y. C. A.; Nieto Faza, O.; Specklin, D.; Jacques, B.; López, C. S.; dos Santos, J. H. Z.; Schrekker, H. S.; Dagorne, S. Acetate-catalyzed hydroboration of CO<sub>2</sub> for the selective formation of methanol-equivalent products. *Catal. Sci. Technol.* **2020**, *10*, 2407–2414.

(9) Tlili, A.; Voituriez, A.; Marinetti, A.; Thuery, P.; Cantat, T. Synergistic effects in ambiphilic phosphino-borane catalysts for the hydroboration of CO<sub>2</sub>. *Chem. Commun.* **2016**, *52*, 7553–7555.

(10) (a) Greenacre, V. K.; Ansell, M. B.; Roe, S. M.; Crossley, I. R. Synthesis, Structures and Coordination Chemistry of Singly Bridged Phosphane-Boranes with Coordinately Unsaturated Platinum Group Metals. *Eur. J. Inorg. Chem.* **2014**, *2014*, 5053–5062. (b) Vergnaud, J.; Grellier, M.; Bouhadir, G.; Vendier, L.; Sabo-Etienne, S.; Bourissou, D. Synthesis and Reactivity of Ruthenium Arene Complexes Incorporating Novel Ph<sub>2</sub>PCH<sub>2</sub>CH<sub>2</sub>BR<sub>2</sub> Ligands. Easy Access to the Four-Membered Ruthenacycle [(*p*-cymene)RuCl( $\kappa^C$ -P-CH<sub>2</sub>CH<sub>2</sub>PPh<sub>2</sub>)]. *Organometallics* **2008**, *27*, 1140–1146. (c) Fischbach, A.; Bazinet, P. R.; Waterman, R.; Tilley, T. D.  $\beta$ -Phosphinoethylboranes as Ambiphilic Ligands in Nickel-Methyl Complexes. *Organometallics* **2008**, *27*, 1135–1139.

(11) (a) Bontemps, S.; Vendier, L.; Sabo-Etienne, S. Ruthenium-catalyzed reduction of carbon dioxide to formaldehyde. *J. Am. Chem. Soc.* **2014**, *136*, 4419–4425. (b) Bontemps, S.; Sabo-Etienne, S. Trapping formaldehyde in the homogeneous catalytic reduction of carbon dioxide. *Angew. Chem., Int. Ed.* **2013**, *52*, 10253–10255. (c) Bontemps, S.; Vendier, L.; Sabo-Etienne, S. Borane-mediated carbon dioxide reduction at ruthenium: formation of C<sub>1</sub> and C<sub>2</sub> compounds. *Angew. Chem., Int. Ed.* **2012**, *51*, 1671–1674.

(12) Espinosa, M. R.; Charboneau, D. J.; Garcia de Oliveira, A.; Hazari, N. Controlling Selectivity in the Hydroboration of Carbon Dioxide to the Formic Acid, Formaldehyde, and Methanol Oxidation Levels. *ACS Catal.* **2019**, *9*, 301–314.

(13) Lang, A.; Nöth, H.; Schmidt, M. Synthesis of Structures of (Acyloxy)boranes. Synthesis of Structures of (Acyloxy)boranes. *Chem. Ber.* **1995**, *128*, 751–762.

(14) Fujiwara, K.; Yasuda, S.; Mizuta, T. Reduction of CO<sub>2</sub> to Trimethoxyboroxine with BH<sub>3</sub> in THF. *Organometallics* **2014**, *33*, 6692–6695.

(15) Knopf, I.; Cummins, C. C. Revisiting CO<sub>2</sub> Reduction with NaBH<sub>4</sub> under Aprotic Conditions: Synthesis and Characterization of Sodium Triformatoborohydride. *Organometallics* **2015**, *34*, 1601–1603.

(16) (a) Beletskaya, I.; Pelter, A. Hydroborations catalysed by transition metal complexes. *Tetrahedron* **1997**, *53*, 4957–5026. (b) Obligacion, J. V.; Chirik, P. J. Earth-abundant transition metal catalysts for alkene hydrosilylation and hydroboration. *Nat. Rev. Chem.* **2018**, *2*, 15–34.